Oxidative stress and inflammation induced by air pollution-derived pm2.5 persist in the lungs of mice after cessation of their sub-chronic exposure

Emeline Barbier, Jessica Carpentier, Ophélie Simonin, Pierre Gosset, Anne Platel, Mélanie Happillon, Laurent Y Alleman, Esperanza Perdrix, Véronique Riffault, Thierry Chassat, et al.

Environment International 181 (2023) 108248

Contents lists available at ScienceDirect

Environment International

journal homepage: www.elsevier.com/locate/envint

Full length article

Oxidative stress and inflammation induced by air pollution-derived $PM_{2.5}$ persist in the lungs of mice after cessation of their sub-chronic exposure

Emeline Barbier [a], Jessica Carpentier [a], Ophélie Simonin [a], Pierre Gosset [b], Anne Platel [a], Mélanie Happillon [a], Laurent Y. Alleman [c], Esperanza Perdrix [c], Véronique Riffault [c], Thierry Chassat [d], Jean-Marc Lo Guidice [a], Sébastien Anthérieu [a,1], Guillaume Garçon [a,*,1]

[a] Univ. Lille, CHU Lille, Institut Pasteur de Lille, ULR4483-IMPECS, France
[b] Service d'Anatomo-pathologie, Hôpital Saint Vincent de Paul, Lille, France
[c] IMT Nord Europe, Institut Mines-Télécom, Univ. Lille, Centre for Energy and Environment, Lille, France
[d] Institut Pasteur de Lille, Plateforme d'Expérimentation et de Haute Technologie Animale, Lille, France

ARTICLE INFO

Handling Editor: Adrian Covaci

Keywords:
Air pollution-derived $PM_{2.5}$
A/JOlaHsd mouse
Lung
Acute/Sub-chronic exposures
Recovery period
Oxidative stress
Inflammation

ABSTRACT

More than 7 million early deaths/year are attributable to air pollution. Current health concerns are especially focused on air pollution-derived particulate matter (PM). Although oxidative stress-induced airway inflammation is one of the main adverse outcome pathways triggered by air pollution-derived PM, the persistence of both these underlying mechanisms, even after exposure cessation, remained poorly studied. In this study, A/JOlaHsd mice were also exposed acutely (24 h) or sub-chronically (4 weeks), with or without a recovery period (12 weeks), to two urban $PM_{2.5}$ samples collected during contrasting seasons (*i.e.*, autumn/winter, AW or spring/summer, SS). The distinct intrinsic oxidative potentials (OPs) of AW and SS $PM_{2.5}$, as evaluated in acellular conditions, were closely related to their respective physicochemical characteristics and their respective ability to really generate ROS over-production in the mouse lungs. Despite the early activation of the nuclear factor erythroid 2-related factor 2 (Nrf2) cell signaling pathway by AW and, in a lesser degree, SS $PM_{2.5}$, in the murine lungs after acute and sub-chronic exposures, the critical redox homeostasis was not restored, even after the exposure cessation. Accordingly, an inflammatory response was reported through the activation of the nuclear factor-kappa B (NF-κB) cell signaling pathway activation, the secretion of cytokines, and the recruitment of inflammatory cells, in the murine lungs after the acute and sub-chronic exposures to AW and, in a lesser extent, to SS $PM_{2.5}$, which persisted after the recovery period. Taken together, these original results provided, for the first time, new relevant insights that air pollution-derived $PM_{2.5}$, with relatively high intrinsic OPs, induced oxidative stress and inflammation, which persisted admittedly at a lower level in the lungs after the exposure cessation, thereby contributing to the occurrence of molecular and cellular adverse events leading to the development and/or exacerbation of future chronic inflammatory lung diseases and even cancers.

1. Introduction

Air pollution is one of the global leading environmental causes of death with more than 7 million premature deaths and loss of millions more healthy years of life every year (Cohen et al. 2017, Lelieveld et al. 2019; WHO, 2022). New global air quality guidelines (AQGs) of the world health organization (WHO) for regulated pollutants, such as particulate matter (PM), ozone (O_3), nitrogen dioxide (NO_2), sulfur dioxide (SO_2), and carbon monoxide (CO), are supported by clear evidence of the harmful effects of air pollution on human health at even lower levels than previously reported (WHO, 2022). Of the air pollutants mentioned above, PM has been identified as the main health risk factor (Beelen et al. 2013, Hamra et al. 2014, Loomis et al. 2013; Pope, 2014; Raaschou-Nielsen et al. 2016; WHO, 2022). Practical evidence gathered through epidemiological studies has shown a strong association between air pollution-derived PM and adverse health effects such as respiratory illnesses including inflammatory diseases such as asthma, acute bronchitis, chronic obstructive pulmonary disease (COPD), and lung cancer

* Corresponding author.
E-mail address: guillaume.garcon@univ-lille.fr (G. Garçon).
[1] SA and GG contribute equally to this work.

https://doi.org/10.1016/j.envint.2023.108248
Received 12 August 2023; Received in revised form 28 September 2023; Accepted 3 October 2023
Available online 12 October 2023

(Piao et al. 2021). The international agency for research on cancer (IARC) has also classified outdoor air pollution and particularly PM as proven human carcinogens (group 1) in 2013 (Loomis et al. 2013).

The sizes of the air pollution-derived PM fractions are defined by their aerodynamic equivalent diameter, thus making it possible to distinguish between coarse particles (*i.e.*, $PM_{10\text{-}2.5}$, smaller than, or equal to, 10 μm, and larger than 2.5 μm), fine particles (*i.e.*, $PM_{2.5}$, smaller than, or equal to, 2.5 μm), and ultrafine particles (*i.e.*, $PM_{0.1}$, smaller than, or equal to, 0.1 μm). PM_{10} was the first fractional dimension subject to EU environmental regulation. However, PM_{10} has progressively received less and less attention from toxicologists. Current health concerns are now focused on smallest particles because of their ability to migrate deeply into the lungs, escape broncho-mucociliary and alveolar clearances, and also possibly translocate into the systemic circulation (Stone et al. 2017). Plenty of *in vitro* and *in vivo* experimental studies have notified the lung adverse health effects induced by air pollution-derived $PM_{2.5}$, mostly through their ability to trigger some critical underlying mechanisms of toxicity such as oxidative stress-induced airway inflammation (Abbas et al. 2009, 2010, 2013, 2016, 2019, Badran et al. 2020a, 2020b, Boudjema et al. 2021, Bocchi et al. 2016, Dergham et al. 2012, 2015, Garçon et al. 2006, Gualtieri et al. 2010, 2011, 2018, Halonen et al. 2015, Leclercq et al. 2016, 2017, 2018, Longhin et al. 2013, 2016, 2020, Rajagopalan et al. 2020, Saint-Georges et al. 2008, 2009, Saleh et al. 2019, Sotty et al. 2019, 2020). However, although some progress has been made during the last decade, a considerable effort will still be required to better identify some typical features of toxicological responses, which could be related to some of the specific characteristics of air pollution-derived PM. Particular attention needs to be paid to the types of toxicological responses they induce, as their knowledge is greatly complicated by the fact that this is a very heterogeneous pollutant that is often poorly described (Perrone et al. 2013).

While the underlying mechanisms of toxicity by which air pollution-derived PM induces its adverse health effects remain to be determined, accumulating evidence has supported that particles produce cell and/or tissue damages firstly through both oxidative and inflammatory responses (Ding et al. 2021). The oxidative stress paradigm in particle toxicology encompasses both primary oxidative effects from the particles or chemical and/or biological components-coated onto particles, as well as secondary oxidative effects through oxidative boost within cells and/or tissues (Sotty et al. 2020). In the strictest form, the oxidative stress paradigm postulates that the toxicological reactivity of a particle can be predicted by its intrinsic oxidative potential (OP), which can be measured in cell-free/abiotic systems (Guascito et al. 2021, 2023). Indeed, OP has been suggested as a toxicological relevant feature of air pollution-derived PM that could provide improved exposure metrics, compared to more conventional particle-metrics such as mass, surface area, or number (Bates et al. 2019). Evaluating the intrinsic OP of particles helps to fill this gap by taking into account the capacity of their chemical and/or biological components to generate reactive oxygen species (ROS) (Crobeddu et al. 2017). However, to date, the link between intrinsic OP and the possible oxidative damage induced by the same particles has not yet been elucidated.

Oxidative stress is frequently considered to be the primary critical underlying mechanism dramatically induced by air pollution-derived PM (Halonen et al. 2015). The nuclear factor erythroid 2 p45-related factor 2 (Nrf2), as the well-known main key regulator of the cellular redox homeostasis, is well-equipped to counteract the redox response and also maintain or recover the critical redox balance within cells and/or tissues (Boudjema et al. 2021, Cho and Kleeberger 2015, Holmström et al. 2016, Jiang et al. 2017, Leclercq et al. 2018, Sotty et al. 2020). Indeed, ROS levels in cells and/or tissues are regulated through sophisticated antioxidant defenses that may be enzymatic [*e.g.*, heme oxygenase 1 (HO-1), superoxide dismutase (SOD), catalase (CAT), glutathione peroxidase (GPx), and glutathione reductase (GR)] or non-enzymatic (*e.g.*, glutathione). Among them are phase II detoxification enzymes [*e.g.*, NAD(P)H quinone dehydrogenase 1 (NQO1), and glutathione-S-transferase (GST)], which have antioxidant, detoxifying and cytoprotective activity. The Nrf2 cell signaling pathway is well-known to play a critical role in preventing PM-induced toxicity by protecting cells and/or tissues against oxidative stress (Sotty et al. 2020).

In order to maintain the essential coordinated molecular responses needed to resolve the unbalanced status in cells and/or tissues, Nrf2 and nuclear factor-kappa B (NF-κB) cell signaling pathways, that regulate the responses against oxidative and inflammatory responses, respectively, must closely interplay (Wardyn et al. 2015). The NF-κB cell signaling pathway, which is known to be induced by oxidative stress, is involved in the initiation of the immune response. The existence of a crosstalk between Nrf2 and NF-κB is now certain and has been shown to be critical for the coordination of molecular responses to deal with disorders following PM exposure (Boudjema et al. 2021, Leclercq et al. 2018, Sotty *et al.* 2020). Nevertheless, during oxidative stress, IκB kinase (IKK) is activated and causes the phosphorylation of IκB, resulting in the release and the nuclear translocation of NF-κB and the transcription of complex cascades of pro-inflammatory mediators (Bellezza *et al.* 2018). Among them, cytokines are low molecular-weight proteins and polypeptides secreted by a variety of cells; they regulate cell growth, differentiation, and immune function, and are closely involved in inflammation and wound-healing. Cytokines include interleukins (ILs), interferons, tumor necrosis factor (TNF), colony-stimulating factor (CSF), chemokines, and growth factors (Branchett and Lloyd 2019). Local inflammatory reaction will be triggered by the cytokines secreted by immune cells and some of these pro-inflammatory mediators can thereafter be translocated into the blood circulation, thereby leading to a systemic inflammation (Wardyn et al. 2015).

Despite the attention paid by the scientific community to the type of toxicological responses depending on the exposure strategy of the *in vitro* and *in vivo* models to air pollution-derived PM, and the delay in studying the underlying mechanisms of toxicity, both these critical questions are still far from being fully resolved. New toxicological researches are also urgently requested to improve the current knowledge about the specific cellular and molecular alterations that occur as a function of the duration of exposure and, in particular, the recovery period after exposure cessation. Only a few pieces of relevant toxicological evidence have yet dissected the reversibility of the cellular and molecular processes related to oxidative stress-induced inflammation (Rajagopalan et al. 2020). It is also really important to consider the issues of air pollution-related adverse health effects by undertaking new toxicological research strategies, integrating a recovery period after exposure cessation, in order to evaluate the reversibility and/or persistence of the underlying mechanisms of toxicity induced by air pollution-derived PM.

In this study, A/JOlaHsd mice were exposed by intranasal instillations, acutely (24 h) or sub-chronically for 4 weeks with or without a recovery period of 12 weeks, to different doses of $PM_{2.5}$ (*i.e.*, 0, 10, 50 or 100 μg/30 μL of sterile saline) collected during two contrasting seasons (*i.e.*, autumn/winter, AW or spring/summer, SS). Hence, in this work, we sought to better evaluate the toxicity of these two $PM_{2.5}$ samples depending on their contrasted season of collection and the possible persistence of the PM induced-underlying mechanisms of toxicity, even after a 12-week recovery period, in the lungs of mice. Firstly, after having physically, chemically and biologically characterize the two $PM_{2.5}$ samples, we aimed to evaluate their intrinsic OPs through the 5-(and-6)-chloromethyl-2′,7′-dichlorodihydrofluorescein diacetate, acetyl ester (CM-H_2DCFDA) acellular assay, the dithiothreitol (DTT) assay, the ascorbic acid (AA) depletion assay, and the glutathione (GSH) oxidation assay. Secondly, attention was focused on the ability of both these AW and SS $PM_{2.5}$ samples to induce oxidative stress and inflammatory responses, and, therefore, to activate some of the well-known related cell signaling pathways in the lungs of mice. To this end, Nrf2-Antioxidant response element (ARE) binding activity, its gene expression, and that of some of its target genes [*i.e.*, *Kelch-like ECH-associated*

protein 1 (*Keap1*), *Nrf2*, *Glutathione peroxidase 1* (*Gpx1)*, *heme oxygenase-1* (*Hmox1*), *NADPH quinone oxidoreductase* (*Nqo1*), *Superoxide dismutase 1* (*Sod1)*, and *Thioredoxin* 1 (*Txn1*)] as well as the activities of antioxidant enzymes [*i.e.*, superoxide dismutase (SOD), glutathione peroxidase (GPx), glutathione reductase (GR), and catalase (CAT)], and glutathione status were evaluated. In addition, oxidative lesions [*i.e.*, 4-hydroxynonenal adduct (4-HNE), 8-*iso*-prostaglandin F2α (8-IsoPF2α), 8-hydroxy-2′-deoxyguanosine (8-OHdG), and carbonylated proteins (CO-PROT)] were investigated. Thereafter, the activation of the NF-κB cell signaling pathway (*i.e.*, NF-κB-DNA binding capacity) and cytokine secretion [*i.e.*, granulocyte macrophage colony-stimulating factor (GM-CSF), Interleukin-1β, 6, 10, 13, and 17A (IL1β, IL6, IL10, IL13, and IL17A), keratinocyte-derived chemokine (KC/CXCL1), monocyte chemoattractant protein 1 (MCP1/CCL2), macrophage inflammatory protein-1 alpha (MIP-1α/CCL3), macrophage inflammatory protein-1β/CCL4 (MIP1b), regulated upon activation, normal T cell expressed and secreted (RANTES), and tumor necrosis factor-alpha (TNFα)] in the lungs, and the cell numeration of the bronchoalveolar lavage fluid (BALF) were studied. Taken together, these results could provide new relevant insights about the underlying mechanisms of toxicity occurring within the lungs of mice acutely or sub-chronically exposed to air pollution-derived $PM_{2.5}$, and particularly their possible persistence after a recovery period (*i.e.*, 12 weeks after the exposure cessation).

2. Materials and methods

2.1. Chemicals

Merck-Millipore (St Quentin-en-Yvelines, France) provided cOmplete™, EDTA-free Protease Inhibitor Cocktail, Phosphatase Inhibitor Cocktail, RIPA buffer, Superoxide Dismutase Activity Assay Kit, Glutathione Peroxidase Cellular Activity Assay Kit, Glutathione Reductase Assay Kit, Catalase Assay Kit, and all the other chemicals. ThermoFisher Scientific (Villebon-sur-Yvette, France) provided chloromethyl derivative of 2′,7′-dichlorodihydrofluorescein diacetate (CM-H_2DCFDA), Pierce™ BCA protein assay kits, and all the other reagents for chemistry, and cellular and molecular biology. Qiagen (Courtaboeuf, France) provided RNeasy Mini Kits and QIAamp DNA Mini Kits. Active Motif (La Hulpe, Belgium) provided Nuclear extract Kits, and TransAM® nuclear factor erythroid 2-related factor 2 (Nrf2) and TransAM® nuclear factor-kappa B (NF-κB) kits. Promega (Charbonnière-les-Bains, France) provided GSH/GSSG-Glo™ assays. Abcam (Cambridge, UK) provided 4-hydroxynonenal (4-HNE) modified bovine serum albumin, rabbit polyclonal anti-4-HNE antibody, Protein Carbonyl Content Assay Kit, 8-*iso*-PGF2 alpha ELISA Kit, and 8-hydroxy-2′-deoxyguonosine (8OHdG) ELISA Kit. MSD technologies (Mesoscale Discovery, Rockville, MD, USA) provided all the reagents for the home-made competitive assay for the quantitation of 4-HNE-protein adducts. BIO-RAD (Steenvorde, France) provided the Bio-Plex Pro Mouse Cytokine 23-Plex Immunoassay.

2.2. Field campaign and $PM_{2.5}$ sampling description

Field campaign and $PM_{2.5}$ sampling description have been already described in details by Leclercq et al. (2017). Briefly, air pollution-derived $PM_{2.5}$ samples were collected during two distinct seasons from April 2013 to July 2013 (*i.e.*, SS) and from November 2013 to April 2014 (*i.e.*, AW), respectively, in the center of Lille (France). The sampling site (50°37′53.2″N; 3°04′31.5″E) is surrounded by medium-sized buildings and located <500 m from a high traffic road (N265) and a large train station. The average $PM_{2.5}$ mass concentrations, measured at a monitoring station from the regional air quality monitoring network, were 16.6 ± 8.4 μg/m^3 and 16.8 ± 10.1 μg/m^3 for the SS and AW seasons, respectively. Collected particles with aerodynamic equivalent diameter between 2.5 μm and 0.18 μm (*i.e.*, only the last 3 stages of the high-volume cascade impactor sampler, also referred as $PM_{2.5}$), were retrieved, weighed, homogenized, and kept at −20 °C until their further use for physical, chemical and biological characterization, and toxicological studies.

2.3. Physical, chemical and biological characterization of $PM_{2.5}$

Physical, chemical, and biological characterizations of $PM_{2.5}$ have been almost fully described in details by Leclercq et al. (2017). The size distributions of the $PM_{2.5}$ samples (*i.e.*, SS and AW $PM_{2.5}$), as evaluated by a Zetasizer Nano ZSP™ (Malvern Instruments SARL, Orsay, France) and expressed in numbers, were 972.5 ± 315.4 nm (7.3 %), and 184.5 ± 93.03 nm (92.7 %)) for the SS season (*i.e.*, SS $PM_{2.5}$), and 993.4 ± 295.9 nm (26.1 %), and 172.3 ± 32.82 nm (79.1 %)) for the AW season (*i.e.*, AW $PM_{2.5}$), respectively (see also supplemental data: Table S1). Metal analyses were performed using inductively coupled plasma-atomic emission spectroscopy (IRIS Intrepid, Thermo-Scientific) and -mass spectrometry (NeXion 300x, Perkin Elmer, Villebon-sur-Yvette, France) according to Alleman et al. (2010) and Mbengue et al. (2014). Elemental compositions showed not only some elements usually associated with natural environment (*e.g.*, Al, Ca, Na, Mg, Ti, Sr), but also so-called anthropogenic elements (*e.g.*, Ba, Cr, Cd, Cu, Fe, Ni, Mn, Pb, Zn) (see also supplemental data: Table S2). Polycyclic aromatic hydrocarbon (PAH) analyses were performed using a high-pressure liquid chromotography Waters 2695 Alliance system (Waters SA, Saint-Quentin-en-Yvelines, France) coupled to a 2475-fluorimetric detector according to Crenn *et al.* (2017). High resolution gas chromatography/high resolution mass spectrometry after accelerated solvent extraction were used to quantify polychlorinated dibenzo-*p*-dioxin and furans (PCDD/Fs) and dioxin-like and marker polychlorinated biphenyls (DL/M−PCBs) (Billet et al. 2007, 2008). Several congeners of PAHs, PCDD/Fs, and DL- and M−PCBs were detected within the two $PM_{2.5}$ samples (see also supplemental data: Table S3). Overall, the concentrations of chemicals were higher in the AW as compared to the SS $PM_{2.5}$ (*i.e.*, ∑inorganic elements: 207,004 *vs* 160,246 μg/g, ∑PAHs: 69.4 *vs* 25.4 μg/g, ∑PCDDs: 13.9 *vs* 11.5 fg/g, ∑PCDFs: 6.37 *vs* 4.45 fg/g, ∑DL-PCBs: 44.5 *vs* 24.3 ng/g, and ∑M−PCBs: 233 *vs* 158 ng/g). The Pierce™ Chromogenic Endotoxin Quant Kit (ThermoFisher scientific) allowed to quantify endotoxins, according to the manufacturer's recommendations. There were higher concentrations of endotoxins in the AW (*i.e.*, 0.59 ± 0.16 EU/μg $PM_{2.5}$) as compared to the SS $PM_{2.5}$ (*i.e.*, 0.37 ± 0.03 EU/μg $PM_{2.5}$).

2.4. Intrinsic OP of $PM_{2.5}$

CM-H_2DCFDA acellular assay: The CM-H_2DCFDA acellular assay was based on the oxidation of the non-fluorescent CM-H_2DCFDA probe by the ROS produced by the particles and its conversion into the fluorescent 2′,7′-dichlorofluorescein (DCF). Briefly, CM-H_2DCFDA probe was dissolved at 0.33 mM in absolute ethanol and then activated by incubation with 10 mM NaOH solution for 30 min in the dark at room temperature. The solution was neutralized with phosphate buffered saline (PBS) without calcium and magnesium. Either AW or SS $PM_{2.5}$, from 10 to 100 μg/mL, were incubated at 37 °C with 20 μM CM-H_2DCFDA in Costar® 96-Well Black Polystyrene Plates. Fluorescence generated by probe oxidation was read every 5 min for 1 h ($\lambda_{ex}/\lambda_{em}$ = 485 nm/520 nm) at 37 °C with Spark® 10 M multimode plate reader (TECAN France SASU, Lyon, France) (Boudjema et al. 2021).

DTT assay: The DTT assay was based on a two-step reaction. In the first step, redox active compounds oxidized DTT to its disulphide form which donated an electron to dissolved molecular oxygen, forming superoxide anion. Superoxides can subsequently comproportionate to hydrogen peroxide and oxygen. The rate of DTT-disulphide formation was proportional to the concentration of redox-active species in the sample when DTT was added in excess. In the second step, the remaining DTT reacted with 5,5′-dithiobis(2-nitrobenzoic acid) (DTNB), to generate DTT-disulphide and 2-nitro-5-thiobenzoic (TNB) that was the reagent monitored spectrophotometrically. The experimental procedure

proposed by Crobeddu et al. (2017) was applied. Briefly, either AW or SS $PM_{2.5}$, from 10 to 100 μg/mL, were incubated with 400 mM DTT (Sigma-Aldrich) for 1 h at 37 °C in 30 mM degassed HEPES buffer in Costar® 96-Well transparent Polystyrene Plates. Thereafter, microplates were centrifuged for 15 min at 3500 g at 4 °C. An aliquot of the supernatant was mixed to an equal volume of 2.5 mM DTNB. Absorbance was read at 405 nm with Spark® 10 M multimode plate reader (TECAN France SASU).

AA depletion assay: The AA depletion assay used ascorbic acid as a simplified model of the synthetic respiratory tract lining fluids: AA was oxidized to dehydroascorbic acid while redox active species were reduced, before transferring an electron to oxygen molecules promoting the formation of ROS. Briefly, either AW or SS $PM_{2.5}$, from 10 to 100 μg/mL, were incubated for 10 min at 37 °C in Costar® 96-Well transparent Polystyrene Plates. After adding 200 μM AA solution, the absorption was read at 265 nm at known time intervals for 1 h with Spark® 10 M multimode plate reader (TECAN France SASU) (Visentin et al. 2016).

GSH oxidation assay: The GSH oxidation assay was based on the oxidation by ROS of the reduced form of glutathione (GSH) into the oxidized form (GSSG). After incubation, both the GSH and GSSG concentrations, and also the glutathione status, were evaluated thanks to the GSH/GSSG-Glo™ assay. The GSH/GSSG-Glo™ Assay was a luminescence-based system to detect and quantify total glutathione (GSH + GSSG concentrations), GSSG concentrations, and GSSG/GSH ratio. The determination of both the GSH and GSSG concentrations is based on the GSH-dependent conversion of a GSH probe, Luciferin-NT, to luciferin by a glutathione S-transferase enzyme, coupled to a firefly luciferase reaction. Light from luciferase depends on the amount of luciferin formed, which in turn depends on the amount of GSH present. Briefly, either AW or SS $PM_{2.5}$, from 10 to 100 μg/mL, were incubated for 4 h at 37 °C in a solution containing physiological concentrations (200 μM) of GSH in PBS at pH 7.4 in Costar® 96-Well white Polystyrene Plates with constant mixing. After incubation, both the GSH and GSSG concentrations, and also the GSSG/GSH ratio status, were determined by monitoring luminescence with Spark® 10 M multimode plate reader (TECAN France SASU). (Boudjema et al. 2021).

2.5. A/JOlaHsd mouse exposure to $PM_{2.5}$

The experiments were approved by the local Institutional Animal Care and Use Committee (*i.e.*, Agreement number: 1A 089 099 3589 1), and all the animal procedures were carried out in accordance with Directive 2010/63/EU for animal experiments and French legal recommendations related to animal studies. Seventy-eight male 10-week-old specific pathogen-free (SPF) A/JOlaHsd mice (weight 20-25 g) were obtained from the Harlan Laboratories (Horsy, The Netherlands). Upon arrival, mice were housed into plastic cages (6 mice/cage) within ventilated racks to conventional animal room and maintained under standard conditions for 2 weeks, having free-access to water and maintenance diet *ad libitum*. After this 2-week acclimatization period, mice were divided into 13 groups (n = 6 mice/groups), 7 and 6 groups being intended for the acute and the sub-chronic strategy of exposure, respectively.

Acute exposure: Acutely exposed mice (*i.e.*, 6 groups, n = 6 mice/groups) were intranasally instilled after a light anesthesia (*i.e.*, isoflurane: induction 2.5 % and maintenance 1.5 %) with $PM_{2.5}$ suspensions as follows: 10, 50 or 100 μg of AW or SS $PM_{2.5}$, respectively, suspended in 30 μL of sterile PBS. Negative control group consisting of 6 healthy control mice has undergone the same light anesthesia but was intranasally instilled only with the vehicle (*i.e.*, 30 μL of sterile PBS). Mice were sacrificed 24 h later by an intraperitoneal administration of a sedative analgesic, xylazine (10 mg/kg), in association with a dissociative anesthetic, ketamine (100 mg/kg), and an exsanguination by intracardiac blood sampling.

Sub-chronic exposure: Sub-chronically exposed mice (*i.e.*, 4 groups, n = 6 mice/groups) were intranasally instilled 3 times/week for 4 weeks (28 days) after a light anesthesia (*i.e.*, isoflurane: induction 2.5 % and maintenance 1.5 %) with $PM_{2.5}$ suspensions as follows: 2 groups with 10 μg of AW $PM_{2.5}$ and 2 groups with SS $PM_{2.5}$, suspended in 30 μL of sterile PBS. Negative control groups (*i.e.*, 2 groups, n = 6 mice/groups) have undergone the same light anesthesia but were intranasally instilled only with the vehicle (*i.e.*, 30 μL of sterile PBS). The two first groups, exposed to each type of $PM_{2.5}$, were sacrificed 24 h later for by an intraperitoneal administration of a sedative analgesic, xylazine (10 mg/kg), in association with a dissociative anesthetic, ketamine (100 mg/kg), and an exsanguination by intracardiac blood sampling. The two other groups, exposed to each type of $PM_{2.5}$, were sacrificed after a 12-week recovery period. The two negative control groups were sacrificed after 24 h and a 12-week recovery period, respectively. The health of the mice was monitored daily and their weights were tracked weekly.

2.6. $PM_{2.5}$-induced toxicological endpoints

The further study of the toxicological endpoints needed the preparation of different mouse lung matrices: (i) bronchoalveolar lavages (BALs) were realized with 2 × 1 mL of sterile PBS before removing lungs from the chest cavity, and immediately frozen at -80 °C for use in further experiments. The BAL fluids (BALFs, 1.8 mL) were immediately placed on ice. Free-lung cells were recovered from the BALF by centrifugation at 300*g* for 10 min at 4 °C, (ii) Nrf2-ARE binding activity, NF-κB-DNA binding activity, antioxidant enzyme activities (*i.e.*, SOD, GPx, GR, and CAT), oxidative lesions (*i.e.*, 4-HNE-protein adducts, 8-IsoP F2α, and CO-PROT), and cytokines (*i.e.*, GMCSF, IL1β, IL6, IL10, IL13, and IL17A, KC/CXCL1, MCP1/CCL2, MIP-1α/CCL3, MIP1b, RANTES, and TNFα) were studied after lung tissue lysis with RIPA buffer supplemented with cOmplete™EDTA-free Protease Inhibitor Cocktail and Phosphatase Inhibitor Cocktail (Merck-Millipore), (iii) mRNA expression profiles [*i.e.*, *Keap1*, *Nrf2*, *Gpx1*, *Hmox1*, *Nqo1*, *Sod1*, and *Txn1*) were studied after total RNA extraction with the miRNeasy Mini Kit (Qiagen), and (iv) 8-OHdG were studied after DNA extraction with the QIAamp DNA Mini Kit (Qiagen).

Nrf2 cell signaling pathway activation and oxidative damage: Firstly, the Nrf2-ARE binding activity was studied using TransAM® NRF2 from Active Motif. Associated gene expressions of some members of the Nrf2 signaling pathway (*i.e.*, *Keap1*, *Nrf2*, *Gpx1*, *Hmox1*, *Nqo1*, *Sod1*, and *Txn1*) were evaluated by RT-qPCR using specific Taqman™ gene expression assays (*Keap1*: Mm00497268_m1, *Nrf2*: Mm00477784_m1, *Gpx1*: Mm00656767_g1, *Hmox1*: Mm00516005_m1, *Nqo1*: Mm01253561_m1, *Sod1*: Mm01344233_g1, *Txn1:* Mm00726847_s1, and *PPIA*: Mm02342430_g1), a StepOnePlus™ Real-Time PCR System, and the Expression Suite Software (ThermoFisher scientific). Secondly, antioxidant enzyme activities (*i.e.*, SOD, GPx, GR, and CAT) were studied using Superoxide Dismutase Activity Assay Kit, Glutathione Peroxidase Cellular Activity Assay Kit, Glutathione Reductase Assay Kit, and Catalase assay kit, according to the manufacturer's recommendations. (Garçon et al., 2001a,b, 2006,) Thirdly, the concentrations of 4-HNE-protein adduct, 8-IsoPF2α, CO-PROT, 8-OHdG, and glutathione status (GSSG/GSH) were studied respectively thanks to a home-made competitive ELISA, based on MSD technologies, using 4-HNE-modified BSA and rabbit polyclonal anti-4-HNE antibody, 8-*iso*-PGF2 alpha ELISA Kits, Protein Carbonyl Content Assay Kit, 8-hydroxy-2′-deoxyguanosine ELISA kit, and GSH/GSSG-Glo™ assay, as published elsewhere (Anthérieu et al., 2017; Blasco et al., 2017; Boudjema et al., 2021; Garçon et al., 2006; Leclercq et al., 2016, 2018,).

BALF cell counts: After cytocentrifugation (300 g for 10 min) to prepare cell differential slides, total cell counts were determined and BALF cell slides were stained with May-Grünwald Giemsa using an automated slide stainer. BALF cells were enumerated (300 cells/sample) to determine differential cell counts. Cytotoxicity of lung tissues and BALF cells was evaluated by the determination of extracellular glucose-6-phosphate dehydrogenase (G6PD) activity in cell-free BALF. The Vybrant cytotoxicity assay detects G6PD activity through a two-step

enzymatic process that leads to the reduction of resazurin into red-fluorescent resorufin. The resulting fluorescence signal is proportional to the activity of G6PD released by cells and/or tissues into the BALF, and this release correlates with the number of dead cells. The fluorescence emission of resorufin ($\lambda_{Abs}/\lambda_{Em}$: 563/587 nm), monitored with a Spark® 10 M multimode plate reader (TECAN France SASU), is beyond the autofluorescence of most biological samples (Leclercq et al. 2016).

NF-κB cell signaling pathway activation and cytokine secretion: The NF-κB-DNA binding activity was studied using TransAM® NF-κB from Active Motif. The concentrations of cytokines/chemokines (*i.e.*, GMCSF, IL1β, IL6, IL10, IL13, IL17A, KC/ CXCL1, MCP1/CCL2, MIP-1α/CCL3, MIP1b/CCL4, RANTES, and TNFα) in the lung lysates were detected by Bio-Plex Pro Mouse Cytokine 23-Plex Immunoassay (Blasco et al. 2017).

2.7. Statistical analysis

Results were expressed as mean values and standard deviations, or as medians and interquartile ranges, and maximum and minimum values. For both the acute and the sub-chronic strategies of exposure, comparisons were performed between data (i) from mice exposed to SS or AW $PM_{2.5}$ and those from negative controls, (ii) from mice exposed to SS and those from AW $PM_{2.5}$, and (iii) from mice exposed for the 12-week recovery period (1MR) and those for the 4-week exposure period (1M). After having checked for the normal distribution of the variables under study, the Student's *t*-test was used to perform statistical analyses (Software: SPSS v28 for windows). Differences with a $p < 0.05$ were considered statistically significant (n = 6; Student *t*-test *versus* negative controls: *: $p < 0.05$, and **: $p < 0.01$; Student *t*-test *versus* SS: $^{\#}$: $p < 0.05$; Student *t*-test *versus* 4-week exposure period (1M): ^{a}: $p < 0.05$, and ^{b}: $p < 0.01$).

3. Results

3.1. Physical, chemical, and biological characteristics of $PM_{2.5}$

Physical, chemical, and biological characterization of both the AW and the SS $PM_{2.5}$ bulk samples have been almost fully reported by Leclercq et al. (2017). Results are also shown as supplemental data (see also: Tables S1, S2, and S3).

3.2. Intrinsic OP of $PM_{2.5}$

Intrinsic OPs of both the SS and AW $PM_{2.5}$ samples were determined according to four analytical methods: the CM-H_2DCFDA acellular assay, the DTT assay, the AA depletion assay, and the GSH oxidation assay (Fig. 1). The intrinsic OPs of AW and SS $PM_{2.5}$, at 10, 50 and 100 μg/mL, were firstly determined through the CM-H_2DCFDA acellular assay, thereby showing a dose-dependent activation of the CM-H_2DCFDA probe in presence of AW, and, more markedly, of SS $PM_{2.5}$, *vs* negative controls ($p < 0.05$; Fig. 1A). Moreover, there was a dose-dependent depletion of the DTT induced by AW, and to a lesser extent, for the two lowest doses, by SS $PM_{2.5}$ ($p < 0.05$; Fig. 1B). Similar results were reported when evaluating the intrinsic OP of the AW $PM_{2.5}$ sample by the AA depletion assay ($p < 0.05$; Fig. 1C). However, the intrinsic OP of the SS $PM_{2.5}$ sample, as evaluated by this assay, showed lower responses, also only statistically significant after the exposure to the highest dose ($p < 0.05$; Fig. 1C). In addition, there were statistically significant increases in the GSSG/GSH ratio, thereby suggesting the dose-dependent oxidation of GSH into GSSG in presence of AW, and, in a lesser degree, of SS $PM_{2.5}$ ($p < 0.05$; Fig. 1D). Taken together, these results closely supported that even if the AW and SS $PM_{2.5}$ samples triggered statistically significantly distinct responses, both of them had really a relatively high intrinsic OP.

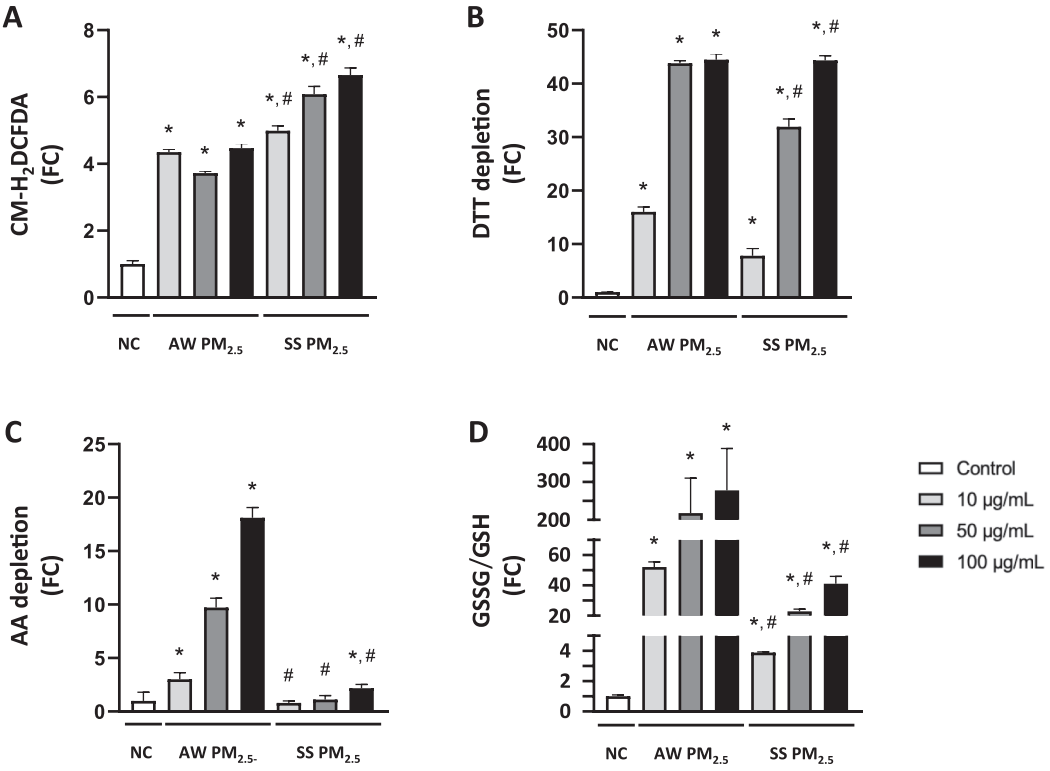

Fig. 1. Intrinsic oxidative potential of the two $PM_{2.5}$ samples collected during two contrasting seasons (*i.e.*, autumn/winter, AW or spring/summer, SS), as determined by chloromethyl derivative of 2′,7′-dichlorodihydrofluorescein diacetate (CM-H_2DCFDA) acellular assay (Fig. 1A), the dithiothreitol (DTT) assay (Fig. 1B), the ascorbic acid (AA) depletion assay (Fig. 1C), and the glutathione (GSH) oxidation assay (Fig. 1D). Values are depicted as mean values and standard deviations (n = 6). Raw values of the negative controls were as follows: CM-H_2DCFDA: 2.05 ± 0.06 RFU; DTT: 5263 ± 533.8 RFU; AA: 0.006 ± 0.005 nmol/L/min; GSSG/GSH: 0.035 ± 0.003 RLU (n = 6; Student *t*-test *versus* negative controls: *: $p < 0.05$, and **: $p < 0.01$; Student *t*-test *versus* SS: $^{\#}$: $p < 0.05$).

3.3. Health monitoring and weight tracking of mice

Health status of acutely and sub-chronically exposed mice was monitored daily. No apparent adverse health effect, behavioral/cognitive deficit, or death was reported 24 h after the acute exposure strategy, or 24 h or 12 weeks after the sub-chronic exposure strategy. Moreover, the weight tracking of the mice was realized 24 h after the acute exposure strategy and weekly for the sub-chronic exposure strategy of 4 weeks and the recovery period of 12 weeks (Fig. 2). There was no significant difference between the weight of the mice acutely exposed to increasing doses of SS or AW $PM_{2.5}$, *vs* negative controls (Fig. 2). No statistically significant loss of weight was reported for the mice sub-chronically exposed to SS or AW $PM_{2.5}$ until the end of the exposure strategy. However, the weight tracking of the mice sub-chronically exposed to SS $PM_{2.5}$ revealed significant losses of weight at the W13, which increased progressively until the end of the exposure strategy, *vs* negative controls (*i.e.*, W13-W15: $p < 0.05$, and W16: $p < 0.01$) (Fig. 2). The weight tracking of the mice sub-chronically exposed to AW $PM_{2.5}$ showed earlier significant reduced weight gain, at the W11, which persisted until the end of the exposure strategy, *vs* the negative controls (*i.e.*, W11-W13: $p < 0.05$, and W14-W16: $p < 0.01$) (Fig. 2). In contrast, no statistically significant reduction of weight gain was reported for the mice sub-chronically exposed to SS $PM_{2.5}$ until the end of the exposure strategy. A slight reduction of weight gain of the mice sub-chronically exposed to SS $PM_{2.5}$ was observed after the 8^{th} and 9^{th} weeks of the recovery period ($p < 0.05$), which was growing progressively until the end of the exposure strategy, *vs* the negative controls (*i.e.*, 10th week: $p < 0.01$, and 11^{th} and 12^{th} weeks: $p < 0.001$) (Fig. 2). No significant difference of weight gain was reported between the mice exposed to the AW *vs* those exposed to SS $PM_{2.5}$.

3.4. $PM_{2.5}$-induced activation of the Nrf2 cell signaling pathway and oxidative damage

Nrf2 cell signaling pathway was significantly activated in a dose-dependent manner in AW, and, to a lesser degree, in SS $PM_{2.5}$-acutely exposed mice, *vs* negative controls (Fig. 3 and Table 1). There were also dose-dependent increases of the Nrf2-ARE binding activity in the lungs of the mice acutely exposed to AW $PM_{2.5}$, from 10 μg/instillation, and, to a lower extend, to SS $PM_{2.5}$, only from 50 μg/instillation, *vs* negative controls ($p < 0.05$) (Fig. 3). Higher increases of the Nrf2-ARE binding activity were generally reported in the lungs of the mice acutely or sub-chronically exposed to AW $PM_{2.5}$ *vs* those exposed to SS $PM_{2.5}$ ($p < 0.05$) (Fig. 3). It is also noteworthy that the increases of the Nrf2-ARE binding activity reported in the lungs of the mice sub-chronically exposed to both the $PM_{2.5}$ samples certainly persisted after the recovery period of

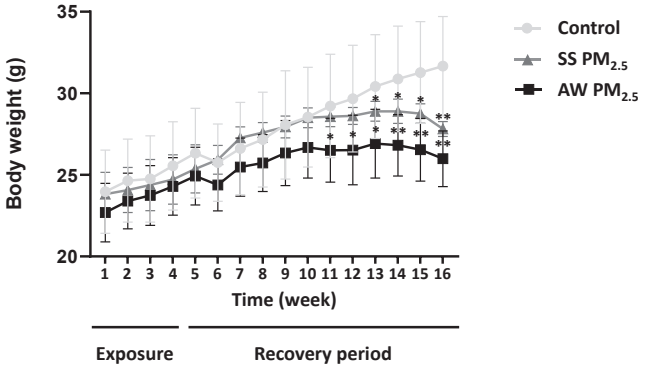

Fig. 2. Weight tracking of the mice 24 h after the acute exposure strategy and weekly for the sub-chronic exposure strategy of 4 weeks and the recovery period of 12 weeks. Values are depicted as mean values and standard deviations (weeks 1 to 4: n =12 and weeks 5 to 16: n = 6). (Student *t*-test *versus* negative controls: *: $p < 0.05$, and **: $p < 0.01$).

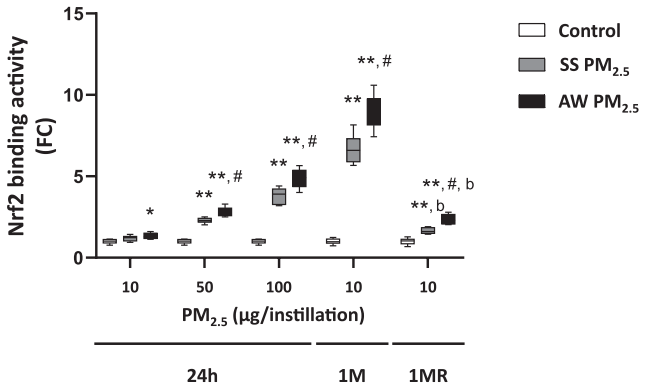

Fig. 3. Binding activity of nuclear factor erythroid 2 p45-related factor 2 (Nrf2) to antioxidant response elements (ARE) in the lungs of the mice 24 h after the acute exposure strategy (24 h), the sub-chronic exposure strategy of 4 weeks (1M), and the recovery period of 12 weeks (1MR) to air pollution-derived particulate matter ($PM_{2.5}$). Values are depicted as medians and interquartile ranges, and maximum and minimum values (n = 6). Raw values of the negative controls were as follows: 24 h: 0.30 ± 0.04 U abs/mg protein, 1M: 0.32 ± 0.05 U abs/mg protein, and 1MR: 0.33 ± 0.07 U abs/mg protein (n = 6; Student *t*-test *versus* negative controls: *: $p < 0.05$, and **: $p < 0.01$; Student *t*-test *versus* SS: $^{\#}$: $p < 0.05$; Student *t*-test *versus* 1M: ^{b}: $p < 0.01$).

12 weeks but with a significantly smaller effect *vs* the exposure period of 4 weeks ($p < 0.01$) (Fig. 3). Moreover, the gene expression of *Nrf2* and some of the downstream target genes, such as *Gpx1*, *Hmox1*, *Nqo1*, *Sod1*, and/or *Txn1*, were significantly up-regulated in the lungs of the mice acutely or sub-chronically exposed to AW and, less markedly, to SS $PM_{2.5}$, *vs* negative controls (Fold change: FC > 1.5, $p < 0.01$) (Table 1). It should be noted that the expression of the *Nrf2* gene and some of the downstream target genes of the Nrf2 cell signaling pathway (*i.e.*, *Gpx1*, *Hmox1*, *Nqo1*, *Sod1*, and *Txn1*) significantly persisted after the 12-week recovery period in the lungs of the mice sub-chronically exposed to AW, and, less markedly, to SS $PM_{2.5}$, but with lower FC values *vs* the 4 week-exposure period (FC > 1.5, p < 0.05) (Table 1). In addition, there were statistically significant increases of GPx and GR enzymatic activities in a dose-dependent manner in the lungs of the mice acutely exposed to AW (from 10 μg/instillation) and, less markedly, to SS $PM_{2.5}$ (from 50 μg/instillation), *vs* negative controls ($p < 0.05$) (Fig. 4B and 4D). Both the GPx and GR enzymatic activities were also increased in the lungs of the mice sub-chronically exposed to both the $PM_{2.5}$ samples ($p < 0.01$). It should be noted that these increases significantly persisted after the 12-week recovery period but with lower enzymatic activities of both the GPx and GR *vs* the 4-week exposure period ($p < 0.05$) (Fig. 4B and 4D). In the same way as for GPx and GR enzymatic activities, there were statistically significant increases of SOD and CAT enzymatic activities in a dose-dependent manner in the lungs of the mice acutely exposed to AW (from 10 μg/instillation) and, to a lesser extent, to SS $PM_{2.5}$ (from 50 μg/instillation), *vs* negative controls (Fig. 4A and 4C). However, somewhat surprisingly, SOD and CAT enzymatic activities were significantly decreased in the lungs of the mice sub-chronically exposed to AW and, less markedly, to SS $PM_{2.5}$, *vs* negative controls ($p < 0.05$) (Fig. 4A and 4C). In contrast, after the recovery period, both these enzymatic activities were slightly but significantly increased in response to the exposure to AW and, in a lesser degree, to SS $PM_{2.5}$ ($p < 0.05$) (Fig. 4A and 4C). Whatever the $PM_{2.5}$ sample under study, significant differences of the enzymatic activities of both the SOD and CAT were also reported between the 4-week exposure period and the 12-week recovery period ($p < 0.01$) (Fig. 4A and 4C). Remarkably, despite the activation of Nrf2 cell signaling pathway, the oxidative alterations of DNA (*i.e.*, 8-OHdG), proteins (*i.e.*, CO-PROT), lipids (*i.e.*, 4-HNE-protein adducts, and 8-Iso-PF2α, data not shown), and glutathione status (*i.e.*, oxidation of GSH into GSSG) occurred in a dose-dependent manner in the lungs of the mice acutely exposed to AW (from 10 μg/instillation) and, to a lesser

Table 1
Lung mRNA expression of some of the genes involved in Nrf2 cell signalling pathway in mice exposed to AW $PM_{2.5}$ or SS $PM_{2.5}$ for 24 h, 1 month (1M) or 1 month with recovery (1MR).

Exposure time	24 h						1M		1MR	
PM dose (μg/instillation)	10		50		100		10		10	
Sampling period	AW	SS	AW	SS	AW	SS	AW	SS	AW	SS
Gpx1	1.43 ± 0.16 **	**1.68 ± 0.17** **	**2.06 ± 0.45** **	**1.92 ± 0.23** **	**2.54 ± 0.62** **	**2.26 ± 0.55** **	**4.34 ± 0.80** **, #	**3.25 ± 0.54** **	**2.29 ± 0.51** **, b	**2.35 ± 1.18** *, b
Hmox1	1.27 ± 0.45	1.40 ± 0.32	**1.54 ± 0.30** **	**1.54 ± 0.49** **	**1.72 ± 0.22** **	**1.68 ± 0.34** **	**3.10 ± 0.64** **, #	**2.57 ± 0.60** **	**1.95 ± 0.32** **, b	**1.82 ± 0.35** **, a
Keap1	**2.30 ± 0.45** **	**1.92 ± 0.38** **	1.01 ± 0.31	1.06 ± 0.30	0.92 ± 0.25	0.95 ± 0.10	1.38 ± 0.33 *	1.35 ± 0.35	1.06 ± 0.06	1.09 ± 0.30 **
Nrf2	**1.53 ± 0.32** **	1.39 ± 0.45	1.47 ± 0.33 *	1.44 ± 0.24 **	1.39 ± 0.33 **	1.48 ± 0.29 **	**4.16 ± 0.46** **, #	**3.07 ± 0.53** **	**1.66 ± 0.17** **, b	**1.54 ± 0.25** **, b
Nqo1	**2.76 ± 0.75** **	**2.24 ± 0.40** **	**3.06 ± 0.63** **	**2.68 ± 0.51** **	**3.66 ± 0.61** **	**3.04 ± 0.60** **	**4.01 ± 0.57** **, #	**2.89 ± 0.56** **	**2.78 ± 0.69** **, #, b	**2.12 ± 0.46** **, a
Sod1	**2.79 ± 0.52** **	**2.44 ± 0.61** **	**3.09 ± 0.70** **	**2.65 ± 0.40** **	**3.74 ± 0.65** **	**3.25 ± 0.76** **	**3.05 ± 0.41** **, #	**2.24 ± 0.60** **	**4.55 ± 0.54** **, #, b	**3.10 ± 0.77** **
Txn1	**3.73 ± 0.65** **	**2.96 ± 0.85** **	**3.88 ± 0.67** **	**3.08 ± 0.81** **	**4.58 ± 0.97** **	**3.29 ± 0.54** **	**3.75 ± 0.67** **, #	**2.65 ± 0.70** **	**2.99 ± 0.48** **, #, b	**2.46 ± 0.32** **

Data are presented as mean values and standard deviations. Gene expressions were calculated by the relative expression ratio of each gene to *PPIA*. AW: autumn–winter and SS: spring-summer (Bold text = Fold change (FC) ≥ 1.5; n = 6; Student *t*-test *versus* negative controls: *: $p < 0.05$, and **: $p < 0.01$; Student *t*-test *versus* SS: #: $p < 0.05$; Student *t*-test *versus* 1M: [a]: $p < 0.05$, and [b]: $p < 0.01$).

degree, to SS $PM_{2.5}$ (from 50 μg/instillation), *vs* negative controls ($p < 0.05$) (Fig. 5A, 5B, 5C, and 5D). Nevertheless, it is noteworthy that AW and, less markedly, SS $PM_{2.5}$-induced oxidative damage to all these critical cell macromolecules were observed in the lungs of the mice sub-chronically exposed ($p < 0.05$) (Fig. 5A, 5B, 5C, and 5D). Overall, higher concentrations of 8-OHdG, CO-PROT, 4-HNE-protein adducts, and 8-IsoPF2α, and alterations of the glutathione status (*i.e.*, GSSG/GSH) were also reported in the lungs of the mice acutely or sub-chronically exposed to AW $PM_{2.5}$ *vs* those exposed to SS $PM_{2.5}$ ($p < 0.05$) (Fig. 5A, 5B, 5C, and 5D). Moreover, it should be emphasized that oxidative damage to all these critical cell macromolecules significantly persisted in the lungs of the mice sub-chronically exposed to AW and, less markedly, to SS $PM_{2.5}$, after the recovery period of 12 weeks *vs* the exposure period of 4 weeks ($p < 0.05$) (Fig. 5A, 5B, 5C, and 5D).

3.5. $PM_{2.5}$-induced activation of the NF-κB cell signaling pathway and inflammatory cell recruitment

As shown in Fig. 6A and 6B, there were statistically significant increases in the NF-κB (p65 and p52)-DNA binding activity in the lungs of the mice acutely exposed to AW, and, less markedly, to SS $PM_{2.5}$, from 10 μg/instillation, *vs* negative controls ($p < 0.05$). There were higher increases of NF-κB (p65 and p52)-DNA binding activity in the lungs of the mice sub-chronically exposed to AW and, less markedly, to SS $PM_{2.5}$, *vs* negative controls ($p < 0.01$) (Fig. 6A and 6B). Moreover, it is noteworthy that there is only significant increase of the NF-κB (p65)-DNA binding activity, and not the NF-κB (p62)-DNA binding activity, in the lungs of the mice sub-chronically exposed to both the $PM_{2.5}$ samples after the recovery period ($p < 0.01$) (Fig. 6A and 6B). However, the NF-κB (p65)-DNA binding activity in the lungs of the mice sub-chronically exposed to AW or SS $PM_{2.5}$ was significantly lower after the recovery period of 12 weeks *vs* the exposure period of 4 weeks ($p < 0.01$) (Fig. 6A). In addition, the concentration profiles of some cytokines (*i.e.*, IL1β, IL6, IL10, KC/CXCL1, MCP1/CCL2, MIP-1α/CCL3, MIP1b/CCL4, and TNFα) were globally identical according to the different exposure strategies to both the $PM_{2.5}$ samples. Indeed, there were statistically significant increases of the concentrations of the cytokines cited above (*i.e.*, TNFα, IL1β, IL6, and IL10: Fig. 7A, 7B, 7C, and 7D, respectively, and KC/CXCL1, MCP1/CCL2, MIP-1α/CCL3, MIP1b/CCL4: data not shown) in the lungs of the mice acutely or sub-chronically exposed to AW $PM_{2.5}$, from 10 μg/instillation, and to SS $PM_{2.5}$, from 10 μg/instillation, *vs* negative controls ($p < 0.05$) (Fig. 7A, 7B, 7C, and 7D). The concentrations of cytokines reported in the lungs of the mice acutely (*i.e.*, IL-6 for 100 μg/instillation) or sub-chronically (*i.e.*, TNFα, IL1β, and IL6) exposed to AW $PM_{2.5}$ were significantly higher *vs* SS $PM_{2.5}$ ($p < 0.05$) (Fig. 7A, 7B, and 7D). It should be noted that the significant increases of the concentrations of all these cytokines persisted after the recovery period of 12 weeks ($p < 0.05$) (Fig. 7A, 7B, 7C, and 7D). Nevertheless, whatever the $PM_{2.5}$ sample under study, some of these cytokines (*i.e.*, TNFα, IL1β, and IL6) were found at lower concentrations in the mice lungs after the 12-week exposure period *vs* the 4-week recovery period ($p < 0.01$) (Fig. 7A, 7B, 7C, and 7D). In contrast, the concentration profiles of other cytokines (*i.e.*, GMCSF, IL13, IL17A, and RANTES) were very similar depending on the different exposure strategies to the two $PM_{2.5}$ samples. Statistically significant increases of the concentrations of all these cytokines were reported only after the higher doses of AW (from 50 μg/instillation) and SS $PM_{2.5}$ (from 50 μg/instillation) in the lungs of the mice acutely exposed, *vs* negative controls ($p < 0.05$) (Fig. 8A, 8B, 8C, and 8D). The concentrations of all these cytokines were also significantly increased in the lungs of the mice sub-chronically exposed to both the $PM_{2.5}$ samples ($p < 0.01$) (Fig. 8A, 8B, 8C, and 8D). It should be noted that the concentrations of some of these cytokines were statistically significantly higher in the lungs of the mice acutely (*i.e.*, IL13, IL17A, and RANTES for 100 μg/instillation) and sub-chronically (*i.e.*, GMCSF, IL13, IL17A, and RANTES) exposed to AW *vs* SS $PM_{2.5}$ ($p < 0.01$) (Fig. 8A, 8B, 8C, and 8D). Whatever the $PM_{2.5}$ sample under study, significantly increases of the concentrations of all these cytokines persisted in the lungs of mice after the recovery period of 12 weeks, but lower concentrations of these cytokines were reported in the mice lungs after the 12-week exposure period *vs* the 4-week recovery

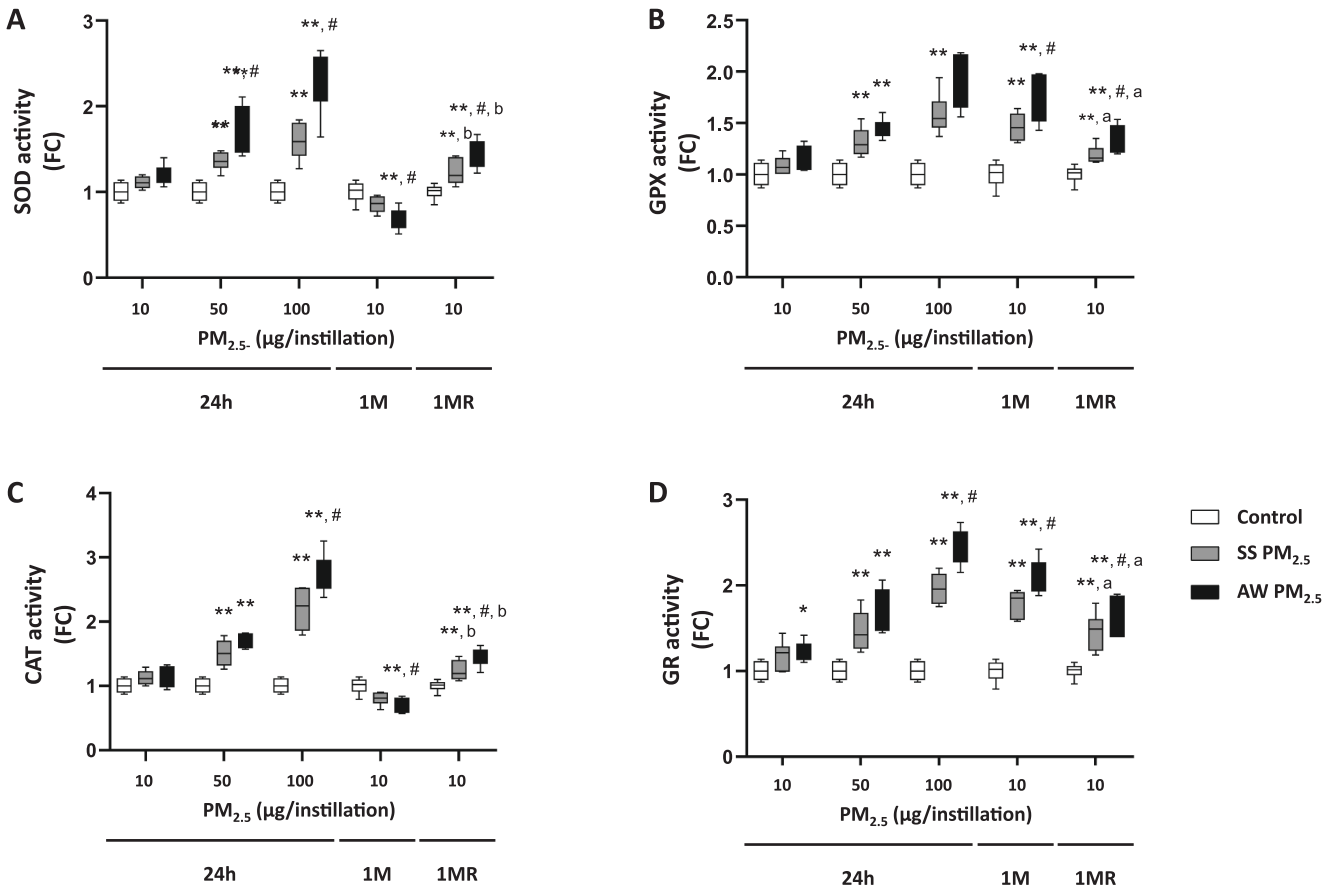

Fig. 4. Enzymatic activities of superoxide dismutase (SOD), glutathione peroxidase (GPx), catalase (CAT), and glutathione reductase (GR) in the lungs of the mice 24 h after the acute exposure strategy (24 h), the sub-chronic exposure strategy of 4 weeks (1M), and the recovery period of 12 weeks (1MR) to air pollution-derived particulate matter ($PM_{2.5}$) (Fig. 4A, 4B, 4C, and 4D, respectively). Values are depicted as medians and interquartile ranges, and maximum and minimum values (n = 6). Raw values of the negative controls were as follows: SOD = 24 h: 657.7 ± 70 mU/mg protein, 1M: 731.4 ± 89.4 mU/mg protein, and 1MR: 703.6 ± 59.3 mU /mg protein; GPx = 24 h: 127.5 ± 14.8 mU/mg protein, 1M: 125.6 ± 15.5 mU/mg protein, and 1MR: 122 ± 14.6 mU /mg protein; CAT = 24 h: 104.6 ± 13.9 mU/mg protein, 1M: 127.3 ± 11.4 mU/mg protein, and 1MR: 121.3 ± 13 mU /mg protein; GR = 24 h: 34.4 ± 8.6 mU/mg protein, 1M: 38.3 ± 7.3 mU/mg protein, and 1MR: 39.1 ± 5.7 mU /mg protein; (n = 6; Student *t*-test *versus* negative controls: *: $p < 0.05$, and **: $p < 0.01$; Student *t*-test *versus* SS: #: $p < 0.05$; Student *t*-test *versus* 1M: [a]: $p < 0.05$, and [b]: $p < 0.01$).

period ($p < 0.01$) (Fig. 8A, 8B, 8C, and 8D). There were statistically significant increases in the BALF total cell count, the polymorphonuclear neutrophils (PMN) and the lymphocytes in the mice acutely (from 50 µg/instillation) and sub-chronically exposed to AW and SS $PM_{2.5}$, *vs* negative controls ($p < 0.01$) (Table 2). Macrophages were significantly less numerous, and, in contrast, PMN and lymphocytes more numerous in the lungs of the mice sub-chronically exposed to AW *vs* SS $PM_{2.5}$ ($p < 0.05$) (Table 2). It should be noted that some of these significant differences persisted after the 12-week recovery period, and were significantly lower *vs* those reported after the 4-week exposure period ($p < 0.05$). In addition, the G6PD activity was statistically significantly increased in the BALF of the mice acutely exposed to AW (*i.e.*, 1.48 and 2.03-fold increases at 50 and 100 µg/instillation, respectively) and, in a lesser extent, SS $PM_{2.5}$ (*i.e.*, 1.38 and 1.78-fold increases at 50 and 100 µg/instillation, respectively), *vs* negative controls (*i.e.*, raw values of the negative controls were as follows: 24 h: 2624.2 ± 311.1 RFU/mg protein) ($p < 0.01$). There were statistically significant increases of the G6PD activity in the lungs of the mice sub-chronically exposed to AW (*i.e.*, 2.42-fold increases) and, less markedly, to SS $PM_{2.5}$ (*i.e.*, 1.57-fold increases), *vs* negative controls (*i.e.*, raw values of the negative controls were as follows: 1 M: 2836.2 ± 239.4 pg/mg protein) ($p < 0.01$). Moreover, it is noteworthy that there were significant increases of the G6PD activity in the lungs of the mice sub-chronically exposed to both the $PM_{2.5}$ samples after the recovery period (*i.e.*, 1.57 and 1.26-fold increases for AW and SS $PM_{2.5}$, respectively) ($p < 0.01$). However, the G6PD activities in the lungs of the mice sub-chronically exposed to AW or SS $PM_{2.5}$ were significantly lower after the 12-week recovery period *vs* the 4-week exposure period (*i.e.*, raw values of the negative controls were as follows: 1MR: 2863 ± 166.8 pg/mg protein) ($p < 0.05$).

4. Discussion

Although the current literature closely supported that the air pollution-derived PM will represent the driving force of this environmental hazard, researchers are still far from having a fully detailed mechanistic explanation for its respiratory toxicity (WHO, 2023). In this work, physically, chemically and biologically characterizing two $PM_{2.5}$ samples collected during two contrasted seasons (*i.e.*, SS and AW), we sought to assess their intrinsic OPs, as toxicological relevant feature that could better predict their toxicological reactivity, thereby improving exposure metrics, compared to more conventional often used particle-metrics. Interestingly, we studied whether the intrinsic OPs of the two $PM_{2.5}$ samples could be correlated to their respective abilities to disrupt, reversibly or not, redox status and inflammatory homeostasis within the lungs of A/JOlaHsd mice, acutely (24 h) or sub-chronically (4-weeks) exposed. One of the relevant highlights of this work was to evaluate the lung persistence of the induced-underlying mechanisms of toxicity, even after a 12-week recovery period.

Two $PM_{2.5}$ samples were collected in an urban surrounding during the two contrasting seasons (*i.e.*, AW or SS). Field campaign and $PM_{2.5}$

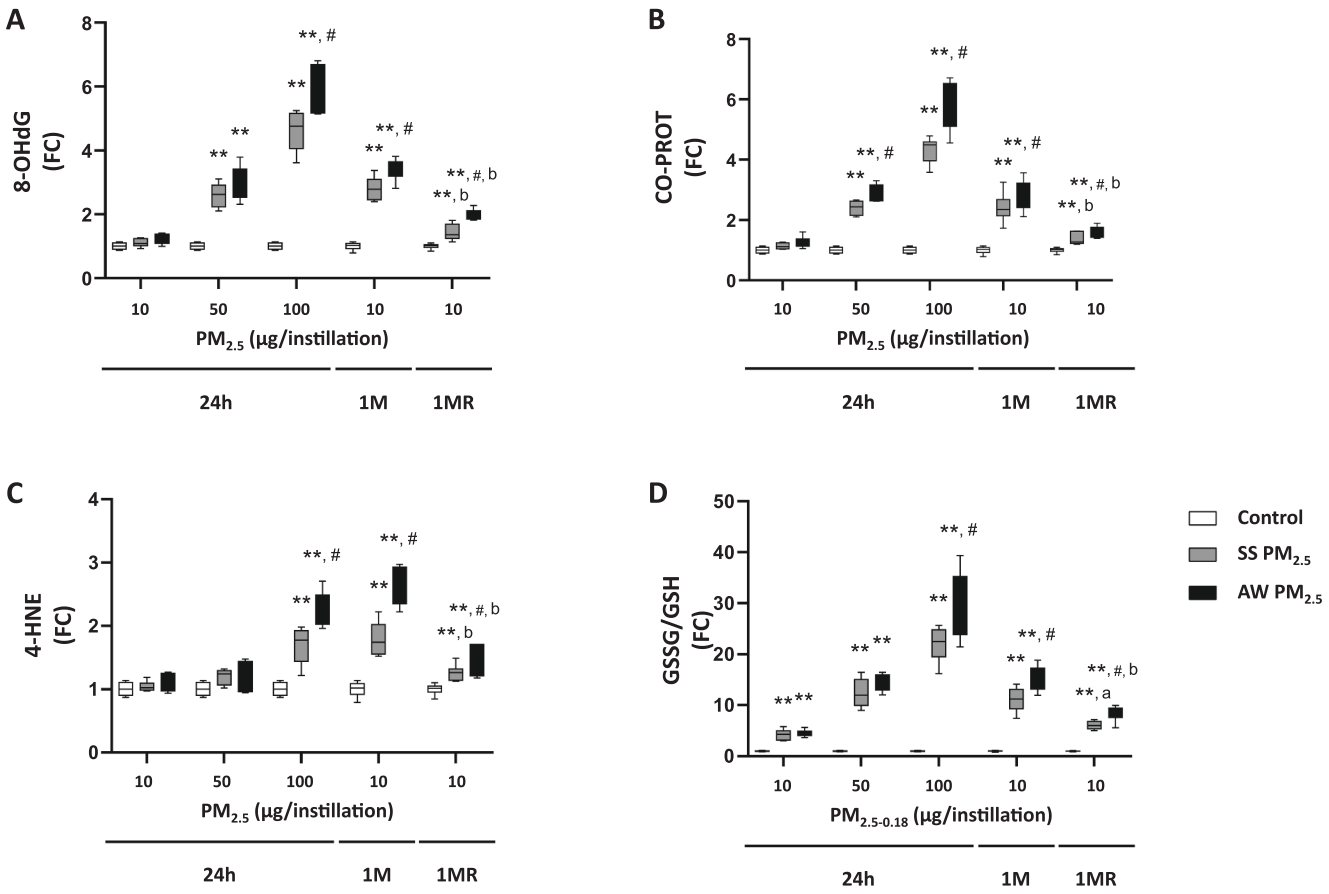

Fig. 5. Concentrations of 8-hydroxy-2′-deoxyguanosine (8-OHdG), carbonylated protein (CO-PROT), 4-hydroxynonenal-protein adducts (4-HNE), and glutathione status (*i.e.*, ratio between the oxidized and the reduced forms, GSSG/GSH) in the lungs of the mice 24 h after the acute exposure strategy (24 h), the sub-chronic exposure strategy of 4 weeks (1M), and the recovery period of 12 weeks (1MR) to air pollution-derived particulate matter ($PM_{2.5}$) (Fig. 5A, 5B, 5C, and 5D, respectively). Values are depicted as medians and interquartile ranges, and maximum and minimum values (n = 6). Raw values of the negative controls were as follows: 8-OHdG = 24 h: 131.5 ± 25.3 pg/µg DNA, 1M: 141.8 ± 18.3 pg/µg DNA, and 1MR: 149.8 ± 19.8 pg/µg DNA; CO-PROT = 24 h: 17.1 ± 2.8 nmol/mg protein, 1M: 19.9 ± 2.7 nmol/mg protein, and 1MR: 21.2 ± 4.9 nmol/mg protein; 4-HNE = 24 h: 1.4 ± 0.3 ng/mg protein, 1M: 1.5 ± 0.2 ng/mg protein, and 1MR: 1.6 ± 0.2 ng/mg protein; GSSG/GSH = 24 h: 0.07 ± 0.02, 1M: 0.1 ± 0.02, and 1MR: 0.11 ± 0.04 (n = 6; Student *t*-test *versus* negative controls: *: $p < 0.05$, and **: $p < 0.01$; Student *t*-test *versus* SS: $^{\#}$: $p < 0.05$; Student *t*-test *versus* 1M: ^{a}: $p < 0.05$, and ^{b}: $p < 0.01$).

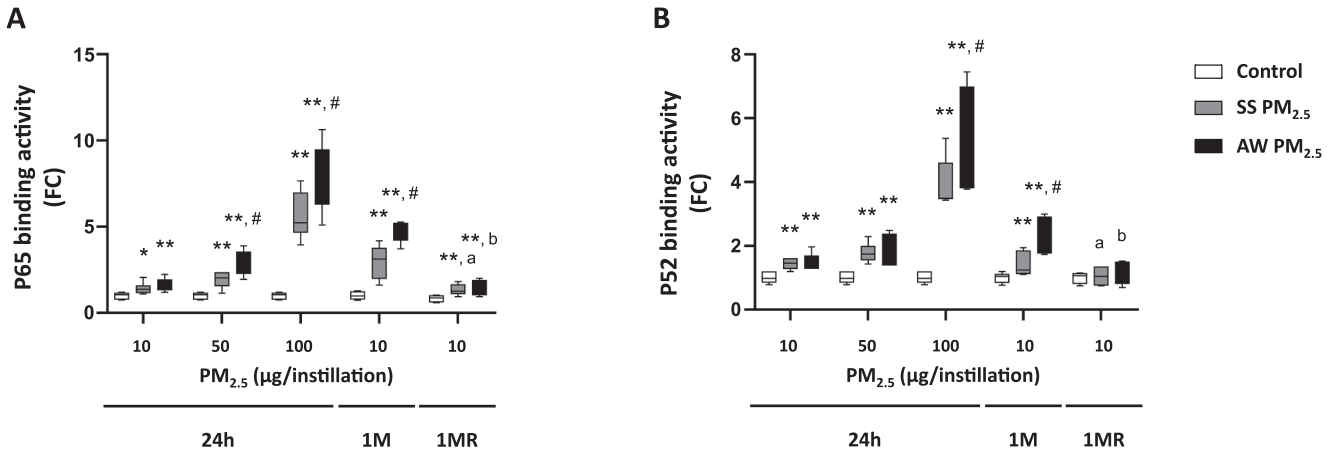

Fig. 6. Binding activity of nuclear factor-kappa B (NF-κB; p65 and p52) to DNA κB motifs in the lungs of the mice 24 h after the acute exposure strategy (24 h), the sub-chronic exposure strategy of 4 weeks (1M), and the recovery period of 12 weeks (1MR) to air pollution-derived particulate matter ($PM_{2.5}$). Values are depicted as medians and interquartile ranges, and maximum and minimum values (n = 6). Raw values of the negative controls were as follows: p65 = 24 h: 0.02 ± 0.01 U abs/mg protein, 1M: 0.04 ± 0.01 U abs/mg protein, and 1MR: 0.03 ± 0.01 U abs/mg protein; p52 = 24 h: 0.02 ± 0.01 U abs/mg protein, 1M: 0.05 ± 0.01 U abs/mg protein, and 1MR: 0.04 ± 0.01 U abs/mg protein (n = 6; Student *t*-test *versus* negative controls: *: $p < 0.05$, and **: $p < 0.01$; Student *t*-test *versus* SS: $^{\#}$: $p < 0.05$; Student *t*-test *versus* 1M: ^{a}: $p < 0.05$, and ^{b}: $p < 0.01$).

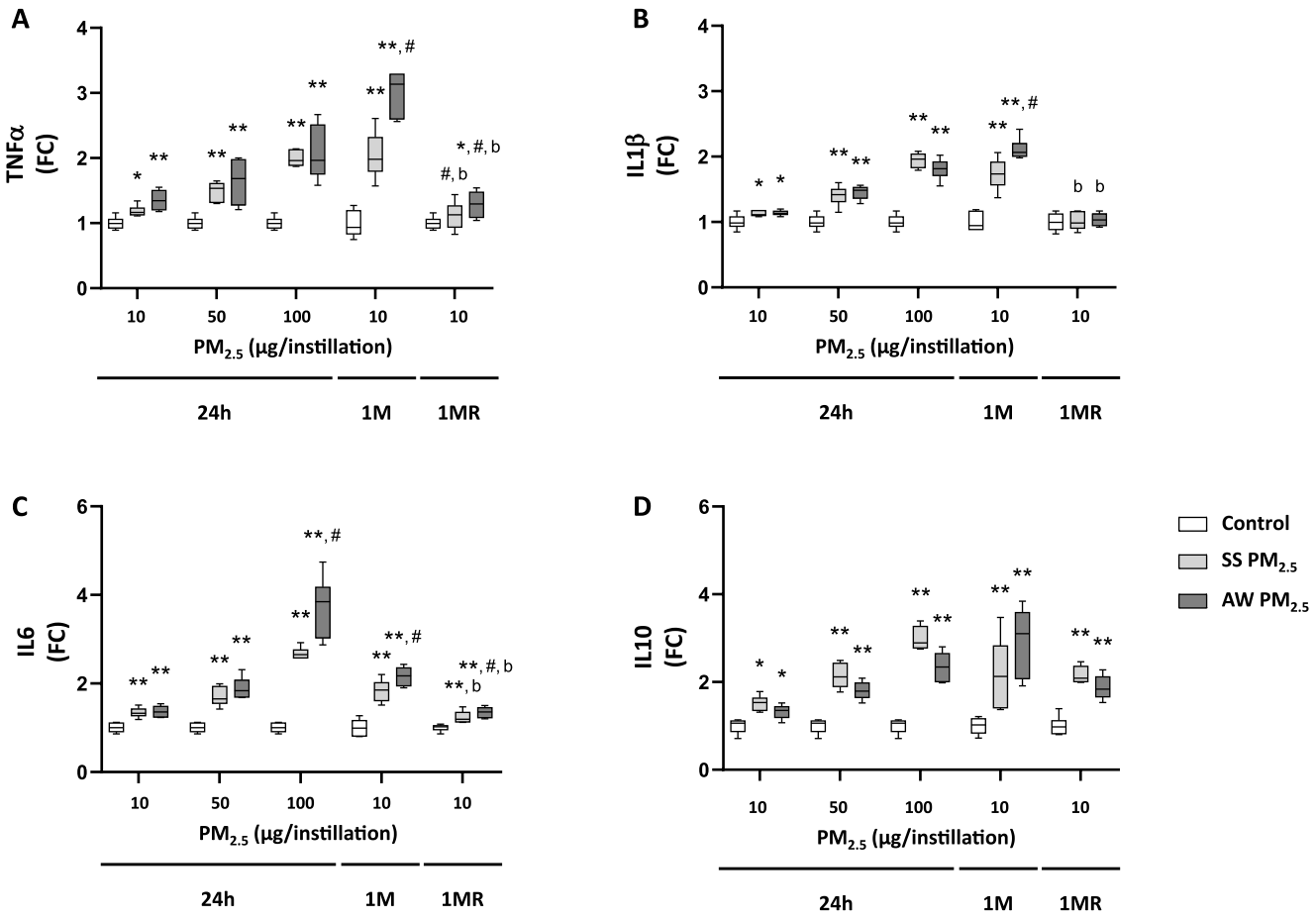

Fig. 7. Concentrations of tumor necrosis factor-alpha (TNFα), Interleukin-1 beta (IL1β), interleukin-6 (IL-6), and interleukin-10 (IL-10) in the lungs of the mice 24 h after the acute exposure strategy (24 h), the sub-chronic exposure strategy of 4 weeks (1M), and the recovery period of 12 weeks (1MR) to air pollution-derived particulate matter ($PM_{2.5}$) (Fig. 7A, 7B, 7C, and 7D, respectively). Values are depicted as medians and interquartile ranges, and maximum and minimum values (n = 6). Raw values of the negative controls were as follows: TNFα = 24 h: 35.66 ± 3.36 pg/mg protein, 1M: 35.23 ± 7.07 pg/mg protein, and 1MR: 30.22 ± 2.84 pg/mg protein; IL1β = 24 h: 54.86 ± 5.83 pg/mg protein, 1M: 55.97 ± 7.85 pg/mg protein, and 1MR: 65.10 ± 8.60 pg/mg protein; IL-6 = 24 h: 3.56 ± 0.40 pg/mg protein, 1M: 14.04 ± 2.57 pg/mg protein, and 1MR: 16.20 ± 1.22 pg/mg protein; IL-10 = 24 h: 2.67 ± 0.43 pg/mg protein, 1M: 2.23 ± 0.41 pg/mg protein, and 1MR: 1.76 ± 0.37 pg/mg protein; (n = 6; Student *t*-test *versus* negative controls: *: $p < 0.05$; **: $p < 0.01$; Student *t*-test *versus* SS: $^{\#}$: $p < 0.05$; Student *t*-test *versus* 1M: ^{b}: $p < 0.01$).

sampling description have been described in details by Leclercq et al. (2017) (*i.e.*, see also supplemental data). The sampling conditions made them likely to be subjected to various emission sources including: secondary inorganic aerosols (37.8 %), biomass combustion (20.6 %), road traffic (14.7 %), coal combustion (8.7 %), soil resuspension (8.1 %), railway (5.3 %), marine (4.8 %), and metallurgy (0.1 %). Among the height identified emission sources, six were mainly local (*i.e.*, on average, 57.4 % of $PM_{2.5}$ mass). Both these $PM_{2.5}$ samples could also be considered as really representative of the air pollution derived-$PM_{2.5}$ impacting the global health of the inhabitants of Lille (France). Since 2015, the European Directive 2008/50/CE defines a 25 µg/m^3 annual mean of $PM_{2.5}$ which must be applied, whereas the WHO recommended a 5 µg/m^3 annual mean of $PM_{2.5}$ to preserve human health (WHO 2023). The mean $PM_{2.5}$ concentrations measured in Lille (*i.e.*, 16.6 ± 8.4 µg/m^3 and 16.8 ± 10.1 µg/m^3 for SS and AW seasons, respectively) were comparable to those found in other Northern French urban areas (Cazier et al. 2016; Crenn et al., 2018; Dergham et al., 2012, 2015). Even if the high-volume cascade impactor sampler exhibited a lower cut-off at 0.39 µm, both the $PM_{2.5}$ samples had a relatively high number of particles below 0.2 µm (*i.e.*, 92.7 % with a mean size of 184.5 nm for SS $PM_{2.5}$ and 73.9 % with a mean size of 172.3 nm for AW $PM_{2.5}$). The concentrations of chemicals were higher in AW as compared to SS $PM_{2.5}$ (*i.e.*, ∑inorganic elements: 207,004 *vs* 160,246 µg/g, ∑PAHs: 69.4 *vs* 25.4 µg/g, ∑PCDDs: 13.9 *vs* 11.5 fg/g, ∑PCDFs: 6.37 *vs* 4.45 fg/g, ∑DL-PCBs: 44.5 *vs* 24.3 ng/g, and ∑M−PCBs: 233 *vs* 158 ng/g). Indeed, the inorganic element concentrations of the two $PM_{2.5}$ samples were comparable to those already reported in the North region of France (Dergham et al. 2012, 2015, Mbengue et al. 2014). Besides, PAH concentrations of the two $PM_{2.5}$ samples were higher than those previously reported from less populated areas of the North region of France (Crenn et al. 2018). The high contribution of combustion particles from vehicle exhaust and unburned fuel could probably explain the relatively high levels of PAHs in AW *vs* SS $PM_{2.5}$ (*i.e.*, 69.4 *vs* 25.4 µg/g). PCDD/Fs and PCBs levels of the two $PM_{2.5}$ samples were in similar ranges of value as those already reported in this region, whereas the levels of DL- and M-PCBs were less important (Dergham et al. 2012, 2015). Finally, there were higher concentrations of endotoxins in AW (*i.e.*, 0.59 ± 0.16 EU/µg) *vs* SS $PM_{2.5}$ (*i.e.*, 0.37 ± 0.03 EU/µg). Overall, given their respective characteristics, both the AW and SS $PM_{2.5}$ samples could have a significant intrinsic OP, and could thereby disrupt the redox status and/or inflammatory homeostasis of target cells, tissues and/or organs (Ding et al. 2021).

In order not to overlook the close relationship between the physico-chemical and toxicological characteristics of both the $PM_{2.5}$, their intrinsic OPs, which can predict their toxicological reactivity, were carefully determined (Bates et al. 2019). In keeping with their respective

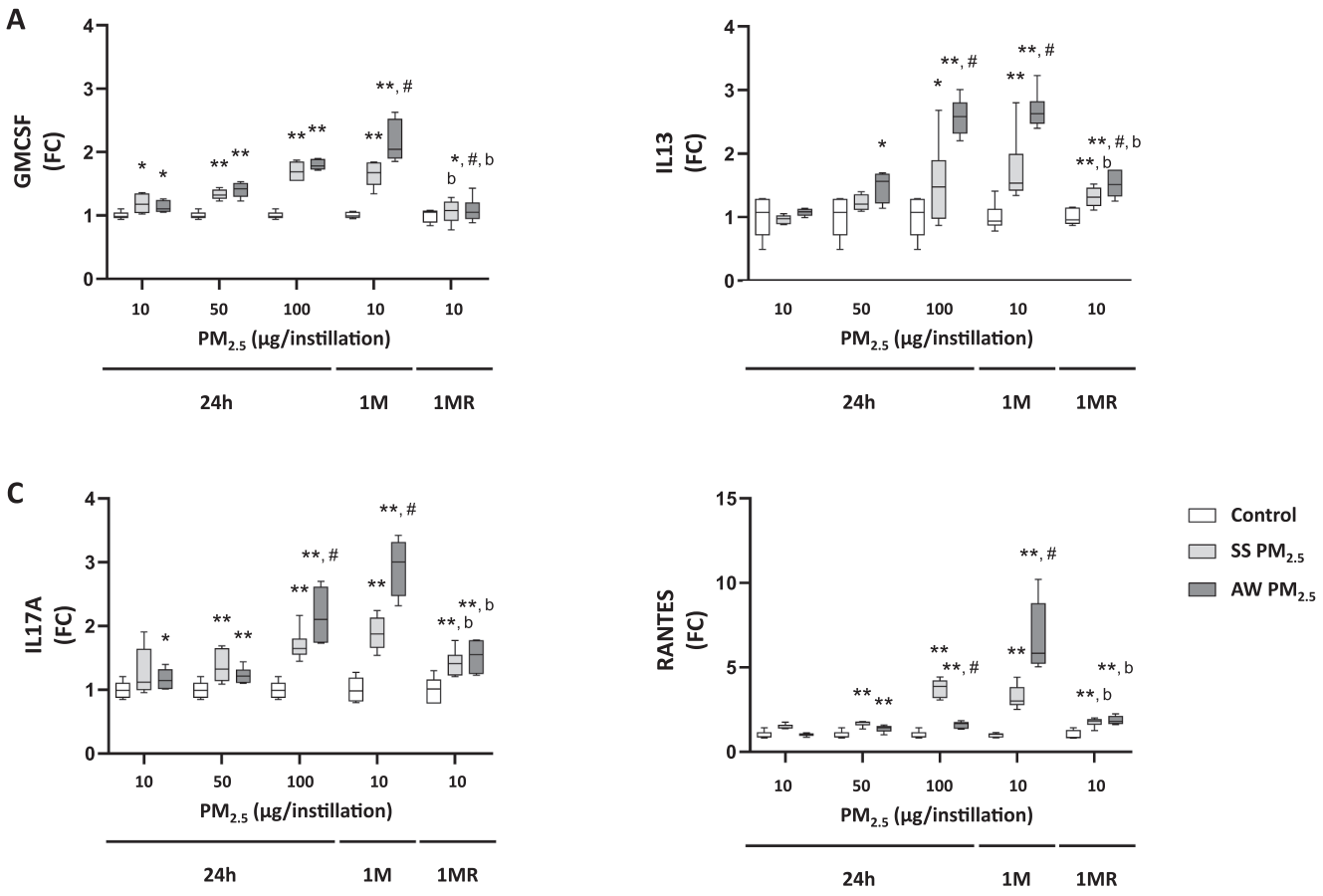

Fig. 8. Concentrations of granulocyte macrophage colony-stimulating factor (GMCSF), interleukin-13 (IL13), interleukin-17A (IL17A), and regulated upon activation, normal T cell expressed and secreted (RANTES), in the lungs of the mice 24 h after the acute exposure strategy (24 h), the sub-chronic exposure strategy of 4 weeks (1M), and the recovery period of 12 weeks (1MR) to air pollution-derived particulate matter ($PM_{2.5}$) (Fig. 8A, 8B, 8C, and 8D, respectively). Values are depicted as medians and interquartile ranges, and maximum and minimum values (n = 6). Raw values of the negative controls were as follows: GMCSF = 24 h: 25.52 ± 1.47 pg/mg protein, 1M: 21.85 ± 0.96 pg/mg protein, and 1MR: 23.05 ± 2.34 pg/mg protein; IL13 = 24 h: 6.26 ± 1.94 pg/mg protein, 1M: 6.37 ± 1.38 pg/mg protein, and 1MR: 5.27 ± 0.65 pg/mg protein; IL17A = 24 h: 8.45 ± 1.14 pg/mg protein, 1M: 6.79 ± 1.32 pg/mg protein, and 1MR: 7.52 ± 1.46 pg/mg protein; RANTES = 24 h: 1.08 ± 0.24 pg/mg protein, 1M: 0.83 ± 0.10 pg/mg protein, and 1MR: 0.84 ± 0.22 pg/mg protein; (n = 6; Student *t*-test *versus* negative controls: *: $p < 0.05$, and **: $p < 0.01$; Student *t*-test *versus* SS: $^{\#}$: $p < 0.05$; Student *t*-test *versus* 1M: ^{b}: $p < 0.01$).

Table 2
Broncho-alveolar liquid fluid (BALF) total cell count in mice exposed to AW $PM_{2.5}$ or SS $PM_{2.5}$ for 24 h, 1 month (1M) or 1 month with recovery (1MR).

Exposure time	24h							1M			1MR		
PM dose (µg/instillation)	0	10		50	50	100		0	10		0	10	
Sampling period		AW	SS	AW	SS	AW	SS		AW	SS		AW	SS
Macrophages (%)	96.52 ± 0.46	96.62 ± 0.34	96.59 ± 0.42	**93.70 ± 0.81****	**94.11 ± 0.73****	**90.15 ± 1.85****	**92.32 ± 1.15****	96.61 ± 0.50	**85.49 ± 1.45**$^{**, \#}$**	**91.04 ± 1.14****	96.80 ± 0.29	**93.56 ± 0.83**$^{**, b}$**	**92.18 ± 0.82****
Polymorphonuclear cells (%)	2.48 ± 0.41	2.02 ± 0.34	2.01 ± 0.23	**3.73 ± 0.69****	**3.39 ± 0.52****	**6.18 ± 1.38****	**4.72 ± 0.89****	2.32 ± 0.48	**10.71 ± 1.53**$^{**, \#}$**	**6.69 ± 0.85****	2.10 ± 0.34	**4.75 ± 0.74**$^{**, b}$**	**6.00 ± 0.76****
Lymphocytes (%)	1.00 ± 0.18	1.35 ± 0.26	1.40 ± 0.31	**2.57 ± 0.26****	**2.50 ± 0.27****	**3.67 ± 0.66****	**2.97 ± 0.38****	1.07 ± 0.30	**3.80 ± 0.52**$^{**, \#}$**	**2.27 ± 0.41****	1.10 ± 0.27	**1.69 ± 0.20**$^{**, \#, b}$**	**1.82 ± 0.33****

Data are presented as mean values and standard deviations. AW: autumn–winter and SS: spring-summer (Bold text = statistically significant differences; n = 6; Student *t*-test *versus* negative controls: *: $p < 0.05$, and **: $p < 0.01$; Student *t*-test *versus* SS: $^{\#}$: $p < 0.05$; Student *t*-test *versus* 1M: ^{b}. $p < 0.01$).

physico-chemical characteristics, results from the four tests used (*i.e.*, CM-H_2DCFDA acellular assay, DTT assay, AA depletion assay, and GSH oxidation assay) closely supported a relatively high intrinsic OPs of AW and SS $PM_{2.5}$ (Crobeddu et al., 2017, 2020). However, the two $PM_{2.5}$ samples showed distinct responses to the 4 tests used, and these differences could be correctly accounted in view of their respective physico-chemical characteristics also described in details in supplemental data. Their specific intrinsic OPs could also be explained by their respective chemical components, namely secondary inorganic ions (*e.g.*, NO_3^-, SO_4^{2-}, NH_4^+), transition metals (*e.g.*, Fe, Cu, Mn, Zn), and organic species (e.g., VOCs, PAHs) (Guo et al. 2017, Gangwar et al. 2020, Pardo et al. 2015, Shuster-Meiseles *et al.* 2016). The current literature recommended the application of different methods to better take into account all the chemical species likely to contribute to the intrinsic OP of PM and the

diversity of their emission sources (Bates *et al.* 2019, Conte et al. 2017, Crobeddu et al. 2020, Fang *et al.* 2016, Janssen et al. 2014). For example, DTT assay and AA depletion assay would be primarily sensitive to transition metals and organic oxygenated species (*e.g.*, quinones), whereas CM-H_2DCFDA acellular assay would only detect certain types of ROS, namely nitryl (°NO_2), hydroxyl (°OH), alkoxyl (RO°), peroxyl (ROO°), peroxynitrites ($ONOO^-$), and peroxides (Charrier and Anastasio 2012, Visentin et al. 2016, Yang et al. 2014, Yu *et al.* 2022). In contrast, GSH oxidation assay would generally detect almost all the ROS, including peroxides, alkanals, protein disulfides, and sulfenic acids (Øvrevik 2019). Overall, despite the distinct responses of the two $PM_{2.5}$ samples under study to the four tests used, our results clearly demonstrated the relatively high intrinsic OPs of both the AW and the SS $PM_{2.5}$, in close relationship with their respective physico-chemical characteristics. However, these relevant data were obtained in cell-free media, highlighting the need to urgently study their toxicological consequences *in vivo*, namely in the murine lungs, thereby helping to fill the crucial gap, that has not been elucidated yet, between the acellular conditions used for the determination of the intrinsic OP and the redox environment of the murine lungs (Crobeddu et al., 2017, 2020).

In this work, male A/JOlaHsd mice were chosen as a murine model because of their specific sensitivity to chemically induced lung tumors, related to their constitutive mutations in the *K-ras* oncogene, and their subsequent frequent uses in toxicological studies on air pollutants (Chen et al. 1994). It is noteworthy that, in this work, the doses of $PM_{2.5}$ acutely (*i.e.*, 10, 50 or 100 μg/instillation) or sub-chronically (*i.e.*, 10 μg/instillation) administrated to mice by intranasal instillation were among the lowest generally used in the current literature (Saleh et al. 2019). The latter presented another interesting aspect since it constituted a somewhat realistic and representative dose of the exposure level of people living in polluted cities during pollution peaks. The PM dose we applied is also among the lowest reported in literature to give significantly harmful effects (Saleh et al. 2019). Indeed, the exposure to 10 μg of air pollution-derived $PM_{2.5}$ would correspond to the exposure to a particle concentration of around 139 μg/m^3 of air for 24 h, which could correspond approximately to the $PM_{2.5}$ concentration very occasionally found during a pollution peak in France (Saleh et al. 2019). This kind of episodes are also possible but, apart some European hotspot, such particle concentrations are reached only very occasionally. Moreover, Manigrasso et al. (2020) recently provided modelling information on the relevance of different PM fractions on the possible doses of the different fraction of the air pollution-derived PM deposited at different target sites, adding relevant information for future setup/interpretation of epidemiological, clinical and toxicological studies. Indeed, in the framework of the 2017 "carbonaceous aerosol in Rome and Environs" (CARE) experiment, particle number size distributions have been continuously monitored in Rome (Italy). These data have been used to estimate, through using the Multiple-Path Particle model Dosimetry model, size and time resolved particle mass, surface area, and number doses deposited into the head, the tracheobronchial, and the alveolar regions of the human respiratory system, thereby supporting expected human lung deposition in the order of few ng/cm^2 of human lung epithelium. It is noteworthy that, considering mice lung epithelial surface, the lowest dose of 10 μg/instillation used in the present work for the 24 h acute exposure period, the 4-week exposure period, and the 12-week recovery period, was in the order of 100 ng/cm^2, and also clearly higher than this expected to be deposited in human lungs. However, it is very important to reduce particle exposure as much as possible, while ensuring a sufficiently high deposited dose in the lungs of mice to study the underlying mechanisms of toxicity, and, at the same time, contributing to the effort to get as close as possible to human exposure levels. Interestingly, in an original way, the 4-week exposure period was followed, or not, by a 12-week recovery period, *i.e.*, a period during which the mice were no longer exposed. The very innovative character of this research was also to consider, through the use of different exposure strategies, whether a recovery period of 12 weeks will be sufficient to evaluate the persistence and/or reversibility of the underlying mechanisms/lesions occurring in lung target cells and/or tissues. It should be noted that, whatever the exposure strategy we applied, the daily monitoring of the health status of mice ensured the lack of any apparent adverse health effect, behavioral/cognitive deficit. However, although there was no alteration of the weight gain during the acute or sub-chronic exposure period, the weight tracking of the mice during the recovery period revealed some statistically significant reductions of weight gain after their exposure to SS and, to a higher extent, to AW $PM_{2.5}$, thereby supporting the persistence of some of the adverse health effects possibly related to $PM_{2.5}$-induced oxidative and/or inflammatory responses within the lungs.

Oxidative stress was also firstly studied. Oxidative stress is also one of the underlying mechanisms generally involved in air pollutant-induced adverse health effects(Abbas et al., 2009, 2010, 2013, 2016, 2019, Badran et al., 2020a,b; Bocchi et al., 2016; Boudjema et al., 2021; Dergham et al., 2012, 2015; Garçon et al., 2006; Gualtieri et al., 2010, 2011, 2018; Halonen et al., 2015; Leclercq et al., 2016, 2017, 2018, Longhin et al., 2013, 2016, 2020; Rajagopalan et al., 2020; Saint-Georges et al., 2008, 2009; Saleh et al., 2019; Sotty et al., 2019, 2020). Hence, after having evaluate the intrinsic OPs of both the $PM_{2.5}$ samples, we sought to investigate if this new particle-metric could be closely correlated to their capacity to alter the redox status in the lungs of mice, acutely (24 h) or sub-chronically (4 weeks) exposed, with a special emphasis on the possible persistence and/or reversibility of oxidative damage, even after a recovery period of 12 weeks. To this end, Nrf2-ARE binding activity, its gene expression and that of some of its target genes as well as the activities of antioxidant enzymes and glutathione status were assessed in the lungs after exposure. Indeed, following exposure to oxidants or electrophiles, Nrf2 accumulates in the nucleus where it binds to ARE in the upstream regulatory regions of genes encoding Nrf2 targets, including antioxidant enzymes, proteins involved in the metabolism and clearance of pollutants, protection against metal toxicity, inhibition of inflammation, repair and removal of damaged proteins, as well as other transcription and growth factors (Suzuki et al. 2016). According to the relatively high intrinsic OPs of both the $PM_{2.5}$, the Nrf2 cell signaling pathway was significantly activated in a dose-dependent manner in AW, and, to a lesser extent, in SS $PM_{2.5}$ acutely and sub-chronically exposed mice. It is very important to highlight that the activation of this critical antioxidant cell signaling pathway still persisted in the murine lungs after the recovery period. Indeed, increases in the Nrf2-ARE binding activity reported in the lungs of the mice sub-chronically exposed to both the $PM_{2.5}$ samples certainly persisted after the recovery period of 12 weeks but with a significantly smaller effect *vs* the exposure period of 4 weeks. Accordingly, the gene expression of *Nrf2* and some of the downstream target genes, such as *Gpx1*, *Hmox1*, *Nqo1*, *Sod1*, and/or *Txn1*, were significantly up-regulated. Some of them were highly supported by the increases and/or decreases of the activities of some of the antioxidant enzymes (*i.e.*, SOD, GPx, GR, CAT) within the lungs of the mice, acutely or sub-chronically exposed to SS and, to a higher extend, AW $PM_{2.5}$, even after the recovery period. It should be noted that all these changes which persisted after the 12-week recovery period were less marked than those reported after the 4-week exposure period. Because of its key role as master regulator of the cell redox homeostasis, Nrf2 is also well-equipped to counteract ROS production and is critical for maintaining the redox balance in the cell (Wardyn et al. 2015). In other *in vitro* and *in vivo* studies, Garçon *et al.* (2001), Leclercq *et al.* (2018) and Sotty *et al.* (2020), studying the NRF2 cell signaling pathway activation within human bronchial epithelial cells repeatedly exposed to air pollution-derived fine or ultrafine particles, clearly supported the key role played by this transcriptional factor to counteract ROS over-production. However, in this work, despite the early effective activation of the Nrf2 cell signaling pathway, massive oxidative damages of DNA (*i.e.*, 8-OHdG), proteins (*i.e.*, CO-PROT), lipids (*i.e.*, 4-HNE-protein adducts, and 8-IsoPF2α, data not shown), and glutathione status (*i.e.*, oxidation of

GSH into GSSG) occurred in a dose-dependent manner in the lungs of the mice acutely or sub-chronically exposed to AW and, to a lesser extent, to SS $PM_{2.5}$. Nevertheless, it is noteworthy that the oxidative damage induced by AW and, less markedly, SS $PM_{2.5}$ in the lungs of the mice sub-chronically exposed, persisted after the recovery period, but with smaller effects. Hence, in this work, because of the inability of the Nrf2 cell signaling pathway to totally ward off the ROS over-production induced by air pollution-derived $PM_{2.5}$, the antioxidant enzymatic and non-enzymatic defenses were exceeded in the lungs of mice acutely and/or sub-chronically exposed. Oxidative damage to DNA, proteins and/or lipids can also disrupt the cell homeostasis, thereby contributing to gene expression deregulation, DNA mutation, protein alteration with loss of function, and lipid peroxidation with loss of membrane integrity and/or fluidity (Abbas et al., 2019; Badran et al., 2020a,b, Garçon et al., 2001a, 2006, Gualtieri et al., 2010, 2011, Leclercq et al., 2016, 2017, 2018, , Longhin et al. 2013, 2016, 2020, Sotty et al. 2020). Other studies have already shown that exposure to air pollution-derived PM could induce oxidative stress, through the catalytic generation of ROS associated with the depletion of antioxidant defense systems, thereby leading to a subsequent imbalance of redox homeostasis (Balakrishna *et al.* 2009, Jelic *et al.* 2021, Lawal 2017, Mazzoli-Rocha et al. 2010, Valavanidis *et al.* 2009, Williams *et al.* 2013). Interestingly, in this work, such an imbalance of redox homeostasis persisted after the 12-week recovery period, even if these oxidative damages were less significant after the recovery period of 12 weeks *vs* the exposure period of 4 weeks. Another highlight of this work was the relationship between the relatively high intrinsic OPs of both the $PM_{2.5}$ samples, evaluated in acellular conditions, and their respective ability to really generate ROS over-production in the mouse lungs. These results also supported the usefulness of the intrinsic OP of PM samples for a better prediction of their toxicological reactivity *in vivo*, thereby improving exposure metrics, compared to more conventional often used particle-metrics (Bates et al. 2019). It is very important to emphasize that, despite the early induction of the Nrf2 cell signaling pathway, in keeping with the relatively high OPs of each of the two $PM_{2.5}$ samples, the redox homeostasis was not restored, even after the exposure cessation, and could also trigger the development and/or the exacerbation of chronic inflammatory and even cancer pathologies in the murine lungs.

Inflammatory homeostasis was secondly studied. Indeed, in order to maintain essential coordinated cellular responses needed to resolve the unbalanced oxidative and/or inflammatory status of the cells and/or tissues, Nrf2 and NFκB cell signaling pathways, that respectively regulate cell signaling pathways related to oxidative stress and inflammation, must closely interplay through multiple molecular interactions, which can often depend on the cell types and tissue contexts (Wardyn et al. 2015). However, in this work, despite the significant increase of the anti-inflammatory Nrf2 binding to ARE, there was a significant activation of the pro-inflammatory NF-κB cell signaling pathway, in the murine lungs acutely or sub-chronically exposed to AW, and, less markedly, SS $PM_{2.5}$. Interestingly, in keeping with the results on intrinsic OPs and oxidative stress, it is noteworthy that there was still significant increase of the NF-κB (p65)-DNA binding activity in the lungs of the mice sub-chronically exposed to both the $PM_{2.5}$ samples after the recovery period, even this significant increase was lower after the recovery period of 12 weeks *vs* the exposure period of 4 weeks. Of course, the activation of the NF-κB cell signaling pathway in the murine lungs whatever the exposure strategy could be closely related to the occurrence of an oxidative stress, itself closely related to their respective chemical components, namely secondary inorganic ions (*e.g.*, NO_3^-, SO_4^{2-}, NH_4^+), transition metals (*e.g.*, Fe, Cu, Mn, Zn), and organic species (e.g., VOCs, PAHs) (Guo et al. 2017, Gangwar et al. 2020, Pardo et al. 2015, Shuster-Meiseles et al. 2016). Moreover, the relatively high concentrations of endotoxins reported in AW and, to a lesser extent, SS $PM_{2.5}$, could rapidly induce a strong pro-inflammatory response mediated by the bronchiolar cells and residential macrophages (Mantecca et al. 2010). Thus, the activation of the NF-κB cell signaling pathway could target inflammation not only directly by increasing the secretion of inflammatory cytokines, chemokines, and adhesion molecules, but also indirectly by regulating cell proliferation, apoptosis, morphogenesis, and differentiation (Liu et al. 2017). Accordingly, the concentration profiles of two sets of pro-inflammatory cytokines (*i.e.*, IL1β, IL6, IL10, KC/CXCL1, MCP1/CCL2, MIP-1α/CCL3, MIP1b/CCL4, and TNFα, on the one hand, and GMCSF, IL13, IL17A, and RANTES, on the other hand) were globally identical whatever the exposure strategies to the two $PM_{2.5}$ samples, and still slightly persisted after the recovery period. In addition, recruitments of inflammatory cells were reported in the murine lungs: there were PMN and lymphocytes influx after the 24 h and 4-week exposures to AW and, in a lesser extent, to SS $PM_{2.5}$, which still slightly persisted after the 12-week recovery period. Accordingly, all these results supported that air pollution-derived $PM_{2.5}$ induced the secretion of some key chemoattractant cytokines in the murine lungs, which could alter the BALF total cell count and cellularity by recruiting PNN, thereby contributing to the development of the inflammatory response (Branchett and Lloyd, 2019; Garçon et al., 2001b; Pardo et al., 2015; Reilly et al., 2019; Rouadi et al., 2020; Valderrama et al. 2022). Another highlight of this work was the development of an inflammatory response in the murine lungs acutely or sub-chronically exposed to AW, and, less markedly, SS $PM_{2.5}$, which slightly persisted, even after the recovery period, and could seriously contribute to the development of chronic inflammatory and even cancer pathologies.

Taken together, these results supported, in a relevant murine model acutely or sub-chronically exposed, the crucial role played by air pollution-derived $PM_{2.5}$, with a relatively high intrinsic OP, in inducing massive oxidative damages to critical cellular macromolecules, despite the Nrf2 cell signaling pathway activation, and in seriously disrupting the inflammatory homeostasis, through the NF-κB cell signaling pathway activation, within the lungs. Moreover, all these results clearly provided, for the first time, new relevant insights about the persistence of both the oxidative stress and the inflammatory conditions after the 12-week recovery period, even at lower levels *vs* the 4-week exposure period, thereby supporting the occurrence of molecular and cellular adverse events contributing to the development and/or exacerbation of future chronic inflammatory lung diseases and even the initiation and/or promotion of lung cancers. These new data clearly raise questions about the health impact of living in an urban environment and the need to urgently adapt current regulations to limit the harmful consequences on populations highly exposed to air pollution-derived PM. They also highlighted the urgent need to better regulate particle emissions in current air quality standards and/or environmental guidelines, as it has been clearly demonstrated that they contribute to a very large part of the human health effects induced by air pollution-derived PM, even after the exposure cessation.

5. Funding sources

This work benefited from grants from the “Institut thématique multi-organisme cancer” (*i.e.*, ITMO Cancer; Plan Cancer 2009–2013, Contract n°ENV201210), the “Conseil Régional du Nord-Pas de Calais” (*i.e.*, Contract n°2013.2543/03), the University of Lille, and IMT Nord Europe. IMT Nord Europe acknowledges financial support from the Labex CaPPA project, which is funded by the French National Research Agency (ANR) through the Programme d’Investissement d’Avenir (PIA) under contract ANR-11-LABX-0005-01, and the CLIMIBIO and ECRIN projects, both financed by the Regional Council “Hauts-de-France” and the European Regional Development Fund (ERDF).

CRediT authorship contribution statement

Emeline Barbier: Methodology, Validation, Formal analysis, Investigation, Writing – original draft. **Jessica Carpentier:** Methodology, Investigation, Validation. **Ophélie Simonin:** Methodology, Investigation, Validation. **Pierre Gosset:** Methodology, Investigation,

Validation. **Anne Platel:** Conceptualization, Investigation, Writing – review & editing. **Mélanie Happillon:** Investigation. **Laurent Y. Alleman:** Methodology, Investigation, Validation, Resources, Writing – review & editing. **Esperanza Perdrix:** Methodology, Investigation, Validation, Resources, Writing – review & editing. **Véronique Riffault:** Methodology, Investigation, Validation, Resources, Writing – review & editing. **Thierry Chassat:** Investigation. **Jean-Marc Lo Guidice:** Methodology, Investigation, Writing – review & editing, Project administration, Funding acquisition. **Sébastien Antherieu:** Methodology, Investigation, Validation, Writing – review & editing, Project administration, Funding acquisition. **Guillaume Garçon:** Conceptualization, Methodology, Investigation, Validation, Resources, Supervision, Writing – original draft, Writing – review & editing, Project administration, Funding acquisition.

Declaration of Competing Interest

The authors declare that they have no known competing financial interests or personal relationships that could have appeared to influence the work reported in this paper.

Data availability

Data will be made available on request.

Appendix A. Supplementary material

Supplementary data to this article can be found online at https://doi.org/10.1016/j.envint.2023.108248.

References

Abbas, I., Saint-Georges, F., Billet, S., Verdin, A., Mulliez, P., Shirali, P., Garçon, G., 2009. Air pollution Particulate Matter ($PM_{2.5}$)-induced gene expression of volatile organic compound and/or polycyclic aromatic hydrocarbon-metabolizing enzymes in an *in vitro* coculture lung model. Toxicol. In Vitro 23 (1), 37–46.

Abbas, I., Garçon, G., Saint-Georges, F., Billet, S., Verdin, A., Gosset, P., Mulliez, P., Shirali, P., 2010. Occurrence of molecular abnormalities of cell cycle in L132 cells after *in vitro* short-term exposure to air pollution $PM_{2.5}$. Chem. Biol. Interact. 188 (3), 558–565.

Abbas, I., Garçon, G., Saint-Georges, F., Andre, V., Gosset, P., Billet, S., Goff, J.L., Verdin, A., Mulliez, P., Sichel, F., Shirali, P., 2013. Polycyclic aromatic hydrocarbons within airborne particulate matter ($PM_{2.5}$) produced DNA bulky stable adducts in a human lung cell coculture model. J. Appl. Toxicol. 33 (2), 109–119.

Abbas, I., Verdin, A., Escande, F., Saint-Georges, F., Cazier, F., Mulliez, P., Courcot, D., Shirali, P., Gosset, P., Garçon, G., 2016. *In vitro* short-term exposure to air pollution $PM_{2.5-0.3}$ induced cell cycle alterations and genetic instability in a human lung cell coculture model. Environ. Res. 147, 146–158.

Abbas, I., Badran, G., Verdin, A., Ledoux, F., Roumie, M., Lo Guidice, J.M., Courcot, D., Garçon, G., 2019. *In vitro* evaluation of organic extractable matter from ambient PM2.5 using human bronchial epithelial BEAS-2B cells: Cytotoxicity, oxidative stress, pro-inflammatory response, genotoxicity, and cell cycle deregulation. Environ. Res. 171, 510–522.

Alleman, L.Y., Lamaison, L., Perdrix, E., Robache, A., Galloo, J.-C., 2010. PM10 metal concentrations and source identification using positive matrix factorization and wind sectoring in a French industrial zone. Atmos. Res. 96 (4), 612–625.

Anthérieu, S., Garat, A., Beauval, N., Soyez, M., Allorge, D., Garçon, G., Lo-Guidice, J.M., 2017. Comparison of cellular and transcriptomic effects between electronic cigarette vapor and cigarette smoke in human bronchial epithelial cells. Toxicol. In Vitro 45 (Pt 3), 417–425.

Badran, G., Ledoux, F., Verdin, A., Abbas, I., Roumie, M., Genevray, P., Landkocz, Y., Lo Guidice, J.-M., Garçon, G., Courcot, D., 2020a. Toxicity of fine and quasi-ultrafine particles: focus on the effects of organic extractable and non-extractable matter fractions. Chemosphere 243.

Badran, G., Verdin, A., Grare, C., Abbas, I., Achour, D., Ledoux, F., Roumie, M., Cazier, F., Courcot, D., Lo Guidice, J.M., Garçon, G., 2020b. Toxicological appraisal of the chemical fractions of ambient fine (PM2.5-0.3) and quasi-ultrafine (PM0.3) particles in human bronchial epithelial BEAS-2B cells. Environ. Pollut. 263(Pt A), 114620.

Balakrishna, S., Lomnicki, S., McAvey, K.M., Cole, R.B., Dellinger, B., Cormier, S.A., 2009. Environmentally persistent free radicals amplify ultrafine particle mediated cellular oxidative stress and cytotoxicity. Part. Fibre Toxicol. 6, 11.

Bates, J.T., Fang, T., Verma, V., Zeng, L., Weber, R.J., Tolbert, P.E., Abrams, J.Y., Sarnat, S.E., Klein, M., Mulholland, J.A., Russell, A.G., 2019. Review of Acellular Assays of Ambient Particulate Matter Oxidative Potential: Methods and Relationships with Composition, Sources, and Health Effects. Environ. Sci. Tech. 53 (8), 4003–4019.

Beelen, R., Raaschou-Nielsen, O., Stafoggia, M. (2013) Effects of long-term exposure to air pollution on natural-cause mortality: an analysis of 22 European cohorts within the multicentre ESCAPE project. The lancet 383:785-795.

Bellezza, I., Giambanco, I., Minelli, A., Donato, R., 2018. Nrf2-Keap1 signaling in oxidative and reductive stress. Biochim. Biophys. Acta 1865 (5), 721–733.

Billet, S., Garçon, G., Dagher, Z., Verdin, A., Ledoux, F., Cazier, F., Courcot, D., Aboukais, A., Shirali, P., 2007. Ambient particulate matter ($PM_{2.5}$): physicochemical characterization and metabolic activation of the organic fraction in human lung epithelial cells (A549). Environ. Res. 105 (2), 212–223.

Billet, S., Abbas, I., Goff, J.L., Verdin, A., André, V., Lafargue, P.-E., Hachimi, A., Cazier, F., Sichel, F., Shirali, P., Garçon, G., 2008. Genotoxic potential of polycyclic aromatic hydrocarbons-coated onto airborne particulate matter ($PM_{2.5}$) in human lung epithelial A549 cells. Cancer Lett. 270 (1), 144–155.

Blasco, H., Garcon, G., Patin, F., Veyrat-Durebex, C., Boyer, J., Devos, D., Vourc'h, P., Andres, C.R., Corcia, P., 2017. Panel of Oxidative Stress and Inflammatory Biomarkers in ALS: A Pilot Study. Can. J. Neurol. Sci. 44 (1), 90–95.

Bocchi, C., Bazzini, C., Fontana, F., Pinto, G., Martino, A., Cassoni, F., 2016. Characterization of urban aerosol: seasonal variation of mutagenicity and genotoxicity of $PM_{2.5}$, PM_1 and semi-volatile organic compounds. Mutat. Res. 809, 16–23.

Boudjema, J., Lima, B., Grare, C., Alleman, L.Y., Rousset, D., Perdrix, E., Achour, D., Anthérieu, S., Platel, A., Nesslany, F., Leroyer, A., Nisse, C., Lo Guidice, J.-M., Garçon, G., 2021. Metal enriched quasi-ultrafine particles from stainless steel gas metal arc welding induced genetic and epigenetic alterations in BEAS-2B cells. NanoImpact. 23.

Branchett, W.J., Lloyd, C.M., 2019. Regulatory cytokine function in the respiratory tract. Mucosal Immunol. 12 (3), 589–600.

Cazier, F., Genevray, P., Dewaele, D., Nouali, H., Verdin, A., Ledoux, F., Hachimi, A., Courcot, L., Billet, S., Bouhsina, S., Shirali, P., Garçon, G., Courcot, D., 2016. Characterisation and seasonal variations of particles in the atmosphere of rural, urban and industrial areas: Organic compounds. J. Environ. Sci. (China) 44, 45–56.

Charrier, J.G., Anastasio, C., 2012. On dithiothreitol (DTT) as a measure of oxidative potential for ambient particles: evidence for the importance of soluble transition metals. Atmos. Chem. Phys. 12 (5), 11317–11350.

Chen, B., You, L., Wang, Y., Stoner, G.D., You, M., 1994. Allele-specific activation and expression of the K-ras gene in hybrid mouse lung tumors induced by chemical carcinogens. Carcinogenesis 15 (9), 2031–2035.

Cho, H.-Y., Kleeberger, S.R., 2015. Association of Nrf2 with airway pathogenesis: lessons learned from genetic mouse models. Arch. Toxicol. 89 (11), 1931–1957.

Cohen, A.J., Brauer, M., Burnett, R., Anderson, H.R., Frostad, J., Estep, K., Balakrishnan, K., Brunekreef, B., Dandona, L., Dandona, R., Feigin, V., Freedman, G., Hubbell, B., Jobling, A., Kan, H., Knibbs, L., Liu, Y., Martin, R., Morawska, L., Pope 3rd, C.A., Shin, H., Straif, K., Shaddick, G., Thomas, M., van Dingenen, R., van Donkelaar, A., Vos, T., Murray, C.J.L., Forouzanfar, M.H., 2017. Estimates and 25-year trends of the global burden of disease attributable to ambient air pollution: an analysis of data from the Global Burden of Diseases Study 2015. Lancet 389 (10082), 1907–1918.

Conte E, Canepari S, Frasca D, Simonetti G., 2017. Oxidative Potential of Selected PM Components. Proceedings 2017, 1(5):108.

Crenn, V., Chakraborty, A., Fronval, I., Petitprez, D., Riffault, V., 2018. Fine particles sampled at an urban background site and an industrialized coastal site in Northern France-Part 2: Comparison of offline and online analyses for carbonaceous aerosols. Aerosol Sci. Tech. 52 (3), 287–299.

Crobeddu, B., Aragao-Santiago, L., Bui, L.C., Boland, S., Baeza, S.A., 2017. Oxidative potential of particulate matter 2.5 as predictive indicator of cellular stress. Environ. Pollut. 230, 125–133.

Crobeddu, B., Baudrimont, I., Deweirdt, J., Sciare, J., Badel, A., Camproux, A.C., Bui, L. C., Baeza-Squiban, A., 2020. Lung Antioxidant Depletion: A Predictive Indicator of Cellular Stress Induced by Ambient Fine Particles. Environ. Sci. Tech. 54 (4), 2360–2369.

Dergham, M., Lepers, C., Verdin, A., Billet, S., Cazier, F., Courcot, D., Shirali, P., Garçon, G., 2012. Prooxidant and proinflammatory potency of air pollution particulate matter ($PM_{0.3\text{-}2.5}$) produced in rural- urban- or industrial surroundings in human bronchial epithelial cells (BEAS-2B). Chem. Res. Toxicol. 25, 904–919.

Dergham, M., Lepers, C., Verdin, A., Billet, S., Cazier, F., Courcot, D., Shirali, P., Garçon, G., 2015. Temporal-spatial variations of the physicochemical characteristics of air pollution particulate matter ($PM_{0.3\text{-}2.5}$) and toxicological effects in human bronchial epithelial cells BEAS-2B. Env Res 137, 256–267.

Ding, H., Jiang, M., Li, D., Zhao, Y., Yu, D., Zhang, R., Chen, W., Pi, J., Chen, R., Cui, L., Zheng, Y., Piao, J., 2021. Effects of real-ambient $PM_{2.5}$ exposure on lung damage modulated by Nrf2-/-. Front. Pharmacol. 12 (662664).

Fang, T., Verma, V., Bates, J.T., Abrams, J., Klein, M., Strickland, M.J., Sarnat, S.E., Chang, H.H., Mulholland, J.A., Tolbert, P.E., Russell, A.G., Weber, R.J., 2016. Oxidative potential of ambient water-soluble $PM_{2.5}$ in the southeastern United States: contrasts in sources and health associations between ascorbic acid (AA) and dithiothreitol (DTT) assays. Atmos. Chem. Phys. 16, 3865–3879.

Gangwar, R.S., Bevan, G.H., Palanivel, R., Das, L., Rajagopalan, S., 2020. Oxidative stress pathways of air pollution mediated toxicity: Recent insights. Redox Biol. 34.

Garçon, G., Garry, S., Gosset, P., Zerimech, F., Martin, A., Hannothiaux, M., Shirali, P., 2001a. Benzo(a)pyrene-coated onto Fe2O3 particles-induced lung tissue injury: role of free radicals. Cancer Lett. 167 (1), 7–15.

Garçon, G., Gosset, P., Garry, S., Marez, T., Hannothiaux, M.H., Shirali, P., 2001b. Pulmonary induction of proinflammatory mediators following the rat exposure to benzo(a)pyrene-coated onto Fe2O3 particles. Toxicol. Lett. 121 (2), 107–117.

Garçon, G., Dagher, Z., Zerimech, F., Ledoux, F., Courcot, D., Aboukais, A., Puskaric, E., Shirali, P., 2006. Dunkerque city air pollution particulate matter-induced cytotoxicity, oxidative stress and inflammation in human epithelial lung cells (L132) in culture. Toxicol. In Vitro 20 (4), 519–528.
Gualtieri, M., Øvrevik, J., Holme, J.A., Perrone, M.G., Bolzacchini, E., Schwarze, P.E., Camatini, M., 2010. Differences in cytotoxicity versus pro-inflammatory potency of different PM fractions in human epithelial lung cells. Toxicol. In Vitro 24 (1), 29–39.
Gualtieri, M., Øvrevik, J., Mollerup, S., Asare, N., Longhin, E., Dahlman, H.-J., Camatini, M., Holme, J.A., 2011. Airborne urban particles (Milan winter-$PM_{2.5}$) cause mitotic arrest and cell death: Effects on DNA mitochondria AhR binding and spindle organization. Mutat. Res. 713 (1–2), 18–31.
Gualtieri, M., Grollino, M.G., Consales, C., Costabile, F., Manigrasso, M., Avino, P., Aufderheide, M., Cordelli, E., Di Liberto, L., Petralia, E., Raschellà, G., Stracquadanio, M., Wiedensohler, A., Pacchierotti, F., Zanini, G., 2018. Is it the time to study air pollution effects under environmental conditions? A case study to support the shift of in vitro toxicology from the bench to the field. Chemosphere 207, 552–564.
Guascito, M.R., Pietrogrande, M.C., Decesari, S., Contini, D., 2021. Oxidative Potential of Atmospheric Aerosols, Oxidative Potential of Atmospheric Aerosols. Atmosphere 12 (5), 531.
Guascito, M.R., Lionetto, M.G., Mazzotta, F., Conte, M., Giordano, M.E., Caricato, R., De Bartolomeo, A.R., Dinoi, A., Cesari, D., Merico, E., Mazzotta, L., Contini, D., 2023. Characterisation of the correlations between oxidative potential and in vitro biological effects of PM_{10} at three sites in the central Mediterranean. J. Hazard. Mater. 448, 130872.
Guo, Z., Hong, Z., Dong, W., Deng, C., Zhao, R., Xu, J., Zhuang, G., Zhang, R., 2017. PM2.5-induced oxidative stress and mitochondrial damage in the nasal mucosa of rats. Int. J. Environ. Res. Public Health 29, 14(2).
Halonen, J.I., Hansell, A.L., Gulliver, J., Morley, D., Blangiardo, M., Fecht, D., Toledano, M.B., Beevers, S.D., Anderson, H.R., Kelly, F.J., Tonne, C., 2015. Road traffic noise is associated with increased cardiovascular morbidity and mortality and all-cause mortality in London. Eur. Heart J. 36 (39), 2653–2661.
Hamra, G.B., Guha, N., Cohen, A., Laden, F., Raaschou-Nielsen, O., Samet, J.M., Vineis, P., Forastiere, F., Saldiva, P., Yorifuji, T., Loomis, D., 2014. Outdoor particulate matter exposure and lung cancer: a systematic review and meta-analysis. Environ. Health Perspect. 122 (9), 906–911.
Holmström, K.M., Kostov, R.V., Dinkova-Kostova, A.T., 2016. The multifaceted role of Nrf2 in mitochondrial function. Curr Opinion Toxicol 1, 80–91.
Janssen, N.A., Yang, A., Strak, M., Steenhof, M., Hellack, B., Gerlofs-Nijland, M.E., Kuhlbusch, T., Kelly, F., Harrison, R., Brunekreef, B., Hoek, G., Cassee, F., 2014. Oxidative potential of particulate matter collected at sites with different source characteristics. Sci. Total Environ. 472, 572–581.
Jelic, M., Mandic, A., Maricic, S., Srdjenovic, B., Jelic, M.D., Mandic, A.D., 2021. Oxidative stress and its role in cancer. J. Cancer Res. Ther. 17 (1), 22–28.
Jiang, Y., Wang, X., Hu, D., 2017. Mitochondrial alterations during oxidative stress in chronic obstructive pulmonary disease. Int. J. COPD 12, 1153–1162.
Lawal, A.O., 2017. Air particulate matter induced oxidative stress and inflammation in cardiovascular disease and atherosclerosis: The role of Nrf2 and AhR-mediated pathways. Toxicol. Lett. 270, 88–95.
Leclercq, B., Happillon, M., Antherieu, S., Hardy, E.M., Alleman, L.Y., Grova, N., Perdrix, E., Appenzeller, B.M., Lo Guidice, J.-M., Coddeville, P., Garçon, G., 2016. Differential responses of healthy and chronic obstructive pulmonary diseased human bronchial epithelial cells repeatedly exposed to air pollution-derived PM_4. Env Poll 218, 1074–1088.
Leclercq, B., Platel, A., Antherieu, S., Alleman, L.Y., Hardy, E.M., Perdrix, E., Grova, N., Riffault, V., Appenzeller, B.M., Happillon, M., Nesslany, F., Coddeville, P., Lo-Guidice, J.-M., Garçon, G., 2017. Genetic and epigenetic alterations in normal and sensitive COPD-diseased human bronchial epithelial cells repeatedly exposed to air pollution-derived $PM_{2.5}$. Env. Poll. 230, 163–177.
Leclercq, B., Kluza, J., Antherieu, S., Sotty, J., Alleman, L.Y., Perdrix, E., Loyens, A., Coddeville, P., Lo Guidice, J.M., Marchetti, P., Garçon, G., 2018. Air pollution-derived $PM_{2.5}$ impairs mitochondrial function in healthy and chronic obstructive pulmonary diseased human bronchial epithelial cells. Environ. Pollut. 243(PtB), 1434–1449.
Lelieveld, J., Klingmüller, K., Pozzer, A., Pöschl, U., Fnais, M., Daiber, A., Münzel, T., 2019. Cardiovascular disease burden from ambient air pollution in Europe reassessed using novel hazard ratio functions. Eur. Heart J. 40 (20), 1590–1596.
Longhin, E., Pezzolato, E., Mantecca, P., Holme, J.A., Franzetti, A., Camatini, M., Gualtieri, M., 2013. Season linked responses to fine and quasi-ultrafine Milan PM in cultured cells. Toxicol. In Vitro 27 (2), 551–559.
Liu, T., Zhang, L., Joo, D., Sun, S.C., 2017. NF-κB signaling in inflammation. Signal Transduct. Target Ther. 2, 17023.
Longhin, E., Capasso, L., Battaglia, C., Proverbio, M.C., Cosentino, C., Cifola, I., Mangano, E., Camatini, M., Gualtieri, M., 2016. Integrative transcriptomic and protein analysis of human bronchial BEAS-2B exposed to seasonal urban particulate matter. Environ. Poll. 209, 87–98.
Longhin, E.M., Mantecca, P., Gualtieri, M., 2020. Fifteen Years of Airborne Particulates in VitroToxicology in Milano: Lessons and Perspectives Learned. Int. J. Mol. Sci. 21 (7), 2489.
Loomis, D., Grosse, Y., Lauby-Secretan, B., El Ghissassi, F., Bouvard, V., Benbrahim-Tallaa, L., Guha, N., Baan, R., Mattock, H., Straif, K., 2013. on behalf of the International Agency for Research on Cancer. Lancet Oncol 14, 1262–1263.
Manigrasso, M., Costabile, F., Liberto, L.D., Gobbi, G.P., Gualtieri, M., Zanini, G., Avino, P., 2020. Size resolved aerosol respiratory doses in a Mediterranean urban area: From PM_{10} to ultrafine particles. Environ. Int. 141, 105714.
Mantecca, P., Farina, F., Moschini, E., Gallinotti, D., Gualtieri, M., Rohr, A., Sancini, G., Palestini, P., Camatini, M., 2010. Comparative acute lung inflammation induced by atmospheric PM and size-fractionated tire particles. Toxicol. Lett. 198 (2), 244–254.
Mazzoli-Rocha, F., Fernandes, S., Einicker-Lamas, M., Zin, W.A., 2010. Roles of oxidative stress in signaling and inflammation induced by particulate matter. Cell Biol. Toxicol. 26 (5), 481–498.
Mbengue, S., Alleman, L.Y., Flament, P., 2014. Size-distributed metallic elements in submicronic and ultrafine atmospheric particles from urban and industrial areas in northern France. Atmos. Res. 135–136, 35–47.
Øvrevik, J., 2019. Oxidative Potential Versus Biological Effects: A Review on the Relevance of Cell-Free/Abiotic Assays as Predictors of Toxicity from Airborne Particulate Matter. Int. J. Mol. Sci. 20 (19), 4772.
Pardo, G., Moral, R., Aguilera, E., Del Prado, A., 2015. Gaseous emissions from management of solid waste: a systematic review. Glob. Chang. Biol. 21 (3), 1313–1327.
Perrone, M.G., Gualtieri, M., Consonni, V., Ferrero, L., Sangiorgi, G., Longhin, E., Ballabio, D., Bolzacchini, E., Camatini, M., 2013. Particle size, chemical composition, seasons of the year and urban, rural or remote site origins as determinants of biological effects of particulate matter on pulmonary cells. Environ. Pollut. 176, 215–227.
Piao, C.H., Fan, Y., Nguyen, T.V., Shin, H.S., Kim, H.T., Song, C.H., Chai, O.H., 2021. $PM_{2.5}$ exacerbates oxidative stress and inflammatory response through the Nrf2/NF-κB signaling pathway in OVA-induced allergic rhinitis mouse model. Int. J. Mol. Sci. 22 (15), 8173.
Pope, C.A. 3rd., 2014. Particulate air pollution and lung function. Am. J. Respir. Crit. Care Med. 190 (5), 485–486.
Raaschou-Nielsen, O., Beelen, R., Wang, M., Hoek, G., Andersen, Z.J., Hoffmann, B., Stafoggia, M., Samoli, E., Weinmayr, G., Dimakopoulou, K., Nieuwenhuijsen, M., Xun, W.W., Fischer, P., Eriksen, K.T., Sørensen, M., Tjønneland, A., Ricceri, F., de Hoogh, K., Key, T., Eeftens, M., Peeters, P.H., Bueno-de-Mesquita, H.B., Meliefste, K., Oftedal, B., Schwarze, P.E., Nafstad, P., Galassi, C., Migliore, E., Ranzi, A., Cesaroni, G., Badaloni, C., Forastiere, F., Penell, J., De Faire, U., Korek, M., Pedersen, N., Östenson, C.-G., Pershagen, G., Fratiglioni, L., Concin, H., Nagel, G., Jaensch, A., Ineichen, A., Naccarati, A., Katsoulis, M., Trichpoulou, A., Keuken, M., Jedynska, A., Kooter, I.M., Kukkonen, J., Brunekreef, B., Sokhi, R.S., Katsouyanni, K., Vineis, P., 2016. Particulate matter air pollution components and risk for lung cancer. Environ. Int. 87, 66–73.
Rajagopalan, S., Park, B., Palanivel, R., Vinayachandran, V., Deiuliis, J.A., Gangwar, R.S., Das, L., Yin, J., Choi, Y., Al-Kindi, S., Jain, M.K., Hansen, K.D., Biswal, S., 2020. Metabolic effects of air pollution exposure and reversibility. J. Clin. Invest. 130 (11), 6034–6040.
Reilly, J.P., Zhao, Z., Shashaty, M.G.S., Koyama, T., Christie, J.D., Lanken, P.N., Wang, C., Balmes, J.R., Matthay, M.A., Calfee, C.S., Ware, L.B., 2019. Low to Moderate Air Pollutant Exposure and Acute Respiratory Distress Syndrome after Severe Trauma. Am. J. Respir, Crit. Care 199 (1), 62–70.
Rouadi, P.W., Idriss, S.A., Naclerio, R.M., Peden, D.B., Ansotegui, I.J., Canonica, G.W., Gonzalez-Diaz, S.N., Rosario Filho, N.A., Ivancevich, J.C., Hellings, P.W., Murrieta-Aguttes, M., Zaitoun, F.H., Irani, C., Karam, M.R., Bousquet, J., 2020. Immunopathological features of air pollution and its impact on inflammatory airway diseases (IAD). World Allergy Organ. J. 13 (10), 100467.
Saint-Georges, F., Abbas, I., Billet, S., Verdin, A., Gosset, P., Mulliez, P., Shirali, P., Garçon, G., 2008. Gene expression induction of volatile organic compound and/or polycyclic aromatic hydrocarbon-metabolizing enzymes in isolated human alveolar macrophages in response to airborne particulate matter $PM_{2.5}$. Toxicology 244 (2–3), 220–230.
Saint-Georges, F., Garçon, G., Escande, F., Abbas, I., Verdin, A., Gosset, P., Mulliez, P., Shirali, P., 2009. Role of air pollution particulate matter ($PM_{2.5}$) in the occurrence of loss of heterozygosity in multiple critical regions of 3p chromosome in human epithelial lung cells L132. Toxicol. Lett. 187 (3), 172–179.
Saleh, Y., Antherieu, S., Dusautoir, R., Alleman, L.Y., Sotty, J., De Sousa, C., Platel, A., Perdrix, E., Riffault, V., Fronval, I., Nesslany, F., Canivet, L., Garçon, G., Lo-Guidice, J.-M., 2019. Exposure to atmospheric ultrafine particles induces severe lung inflammatory response and tissue remodeling in mice. Int. J. Environ. Res. Public Health 16 (7), 1210.
Shuster-Meiseles, T., Shafer, M.M., Heo, J., Pardo, M., Antkiewicz, D.S., Schauer, J.J., Rudich, A., Rudich, Y., 2016. ROS-generating/ARE-activating capacity of metals in roadway particulate matter deposited in urban environment. Environ. Res. 146, 252–262.
Sotty, J., Garçon, G., Denayer, F.-O., Alleman, L.-Y., Saleh, Y., Perdrix, E., Riffault, V., Dubot, P., Lo-Guidice, J.-M., Canivet, L., 2019. Toxicological effects of ambient fine ($PM_{2.5\text{-}0.18}$) and ultrafine (PM0.18) particles in healthy and diseased 3D organo-typic mucocilary-phenotype models. Environ. Res. 176.
Sotty, J., Kluza, J., De Sousa, C., Tardivel, M., Anthérieu, S., Alleman, L.-Y., Canivet, L., Perdrix, E., Loyens, A., Marchetti, P., Lo Guidice, J.-M., Garçon, G., 2020. Mitochondrial alterations triggered by repeated exposure to fine ($PM_{2.5\text{-}0.18}$) and quasi-ultrafine (PM0.18) fractions of ambient particulate matter. Environ. Int. 142.
Stone, V., Miller, M.R., Clift, M.J.D., Elder, A., Mills, N.L., Møller, P., Schins, R.P.F., Vogel, U., Kreyling, W.G., Alstrup Jensen, K., Kuhlbusch, T.A.J., Schwarze, P.E., Hoet, P., Pietroiusti, A., De Vizcaya-Ruiz, A., Baeza-Squiban, A., Teixeira, J.P., Tran, C.L., Cassee, F.R., 2017. Nanomaterials versus ambient ultrafine particles: an opportunity to exchange toxicology knowledge. Environ. Health Perspect. 125 (10), 106002.
Suzuki, M., Otsuki, A., Keleku-Lukwete, N., Yamamoto, M., 2016. Overview of redox regulation by Keap1–Nrf2 system in toxicology and cancer. Curr Opinion Toxicol 1, 29–36.

Valavanidis, A., Vlachogianni, T., Fiotakis, C., 2009. 8-hydroxy-2′-deoxyguanosine (8-OHdG): A Critical Biomarker of Oxidative Stress and Carcinogenesis. J. Environ. Sci. Health C 27 (2), 120–139.

Valderrama, A., Ortiz-Hernández, P., Agraz-Cibrián, J.M., Tabares-Guevara, J.H., Gómez, D.M., Zambrano-Zaragoza, J.F., Taborda, N.A., Hernandez, J.C., 2022. Particulate matter (PM10) induces in vitro activation of human neutrophils, and lung histopathological alterations in a mouse model. Sci. Rep. 12 (1), 7581.

Visentin, M., Pagnoni, A., Sarti, E., Pietrogrande, M.C., 2016. Urban $PM_{2.5}$ oxidative potential: Importance of chemical species and comparison of two spectrophotometric cell-free assays. Environ. Pollut. 219, 72–79.

Wardyn, J.D., Ponsford, A.H., Sanderson, C.M., 2015. Dissecting molecular cross-talk between Nrf2 and NF-κB response pathways. Biochem. Soc. Trans. 43, 621–626.

Williams, K.M., Franzi, L.M., Last, J.A., 2013. Cell-Specific Oxidative Stress and Cytotoxicity after Wildfire Coarse Particulate Matter Instillation into Mouse Lung. Toxicol. Appl. Pharmacol. 266 (1), 48–55.

World health Organization (2022) Ambient (outdoor) air pollution https://www.who.int/news-room/fact-sheets/detail/ambient-(outdoor)-air-quality-and-health (09/27/2023).

World health Organization (2023) https://www.eea.europa.eu/publications/status-of-air-quality-in-Europe-2022/europes-air-quality-status-2022/world-health-organization-who-air (09/27/2023).

Yang, A., Jedynska, A., Hellack, B., Kooter, I., Hoek, G., Brunekreef, B., Kuhlbusch, T.A. J., Cassee, F.R., Janssen, N.A.H., 2014. Measurement of the oxidative potential of $PM_{2.5}$ and its constituents: The effect of extraction solvent and filter type. Atmos. Environ. 83, 35–42.

Yu, Q., Chen, J., Qin, W., Ahmad, M., Zhang, Y., Sun, Y., Xin, K.e., Ai, J., 2022. Oxidative potential associated with water-soluble components of $PM_{2.5}$ in Beijing: The important role of anthropogenic organic aerosols. J. Hazard. Mater. 433.